NONPERTURBATIVE RENORMALIZATION IN CLASSICAL φ^4 THEORY

BY

ANTHONY HEGG

DISSERTATION

Submitted in partial fulfillment of the requirements
for the degree of Doctor of Philosophy in Physics
in the Graduate College of the
University of Illinois at Urbana-Champaign, 2016

Urbana, Illinois

Doctoral Committee:

Professor David Ceperley, Chair
Professor Philip Phillips, Director of Research
Professor Anthony Leggett
Professor Lance Cooper

Abstract

This is an in-depth study of two analytic nonperturbative renormalization group methods used to study nonrelativistic quartic interacting systems. The model studied is that of classical real scalar φ^4 theory. A variety of techniques are used including a rescaling of a nonlinear complete basis, a limit of finite periodic systems, and an analytic calculation of RG equations using a limit of finite systems. Assuming that the truncated forms of the action employed do not change the physics and that standard scaling techniques can be transcribed from more conventional RG approaches to these truncated forms, key results are a new fixed point at strong coupling with exponents $\nu = \frac{2}{d}$ and $\eta = 2 - \frac{d}{2}$ as well as a nonperturbative generation of RG equations and subsequent solution to reduced φ^4 theory. A nontrivial critical point for $d = 3$ is identified in this reduced model with $\nu = 4/(1 + \sqrt{41}) \approx 0.540$ and $\eta = 0$.

To my four Parents for getting me to this point and my Wife for keeping me there.

Acknowledgments

This project would not have been possible without the support of many people. Many thanks to my adviser, Philip W. Phillips. This entire work started with an idea he had at a conference in Europe several years ago and brought up in a group meeting peaking my interest. I subsequently found literature researching that idea in depth several decades ago and then started down a long path to solve the more general version of that idea presented here. Also thanks to my committee members, David Ceperley, Anthony Leggett, and Lance Cooper, for their support and frequent guidance in person or otherwise and regardless of their committee status at the time. A special thanks to my friend and peer Braden Brinkman for letting me bounce ideas around and for helping me crunch through math issues. Thanks to the University of Illinois Graduate College for awarding me a Dissertation Completion Fellowship, providing me with the financial means to complete this project. And finally, thanks to my wife, parents, and numerous friends who endured this long process with me, always offering support and love and putting up with my tendency to give long impromptu seminars on this work and others.

Table of Contents

List of Tables

List of Figures

List of Abbreviations

RG	Renormalization Group.
RSRG	Real-Space Renormalization Group.
BH	Bose-Hubbard Hamiltonian.
SCFP	Strongly Coupled Fixed Point.
LoFS	Limit of Finite Systems.
WLOG	Without Loss of Generality

List of Symbols

φ	a field.
g	the interaction strength.
r	the quadratic coefficient.
p	a momentum magnitude.
k	alternative momentum magnitude.
Λ	the momentum cutoff magnitude.
b	the dimensionless rescaling parameter.
L	a single axis length.
L^d	the volume of a d-dimensional torus.

Chapter 1

A Brief Introduction to Quartic Models

1.1 The Complications of Interactions

We need a new approach to field theory. One that represents the infinite continuum limit of the most prevalent microscopic models in classical, high energy, and condensed matter physics. However, it must be able to access arbitrary interaction strengths without introducing additional perturbative assumptions or numerical approximations. From a statistical mechanical perspective we are interested in calculating properties of the partition function given a suitable Hamiltonian or Lagrangian. Inclusion of quartic interactions in an otherwise free particle Hamiltonian comprises the most ubiquitous models studied in contemporary physics, especially condensed matter physics [2, 13, 14, 18, 39].

Of these, one of the most studied is the classical real scalar φ^4 theory, see e.g. [21]. In particular it is found that the critical point of this system in $d = 3$ dimensions captures the continuous phase transition observed in many fluidic [19], magnetic [19, 44], and even metal-insulator (Mott) [7] systems quite well. Despite decades of research devoted to this model, an analytic nonperturbative calculation of the dominant critical properties remains elusive much less an exact solution to the model itself [12,32]. This situation is indicative of a more widespread and deeply ingrained problem facing physics. There are currently a multitude of experimental systems uncovering a vast array of physical phenomena, but unifying analytic calculations that once-and-for-all can account for the majority of seemingly related observations are extremely rare. Instead, there seem to be as many distinct theoretical and numerical pursuits as there are observed phenomena.

It is likely that in large part the lack of unifying theoretical results stems from the complex difficulties that underlie the systems currently under study. Many of these systems are strongly interacting and often also deliberately rendered inhomogeneous such as via doping, using heterostructure fabrication methods, performing extreme quenching, etc. The latter create a far more rich space of materials to study and utilize, but these augmentations do not necessarily destroy the underlying physical similarity that many of these systems are expected to share [39].

Further, our understanding of relatively homogeneous strongly interacting systems can be said to be lack-

ing [4]. Many successful efforts to calculate physical observables in such strongly interacting systems rely on either perturbative analytics or numerical approximations. Both of these treatments have helped understand and predict such systems to an extent, but this understanding is limited in comparison to the hypothetical knowledge gained by an exact analytical treatment of the same physical observables. Perturbative analysis can capture the exact theoretical framework underlying weakly interacting systems, but there are examples showing that such a particle-like picture is likely to breakdown for stronger interactions [8]. In order to have a chance at unifying the components of such models that lead to similar behavior in seemingly different physical systems we would need a distinctly nonperturbative analytic approach. One that is general enough to be applicable to classical and quantum systems alike. We identify strong candidates for such an approach and utilize them to gain a deeper understanding of the mechanism behind strongly coupled systems. We will elucidate the components of these nonperturbative analytic methods using the classical scalar φ^4 theory as the simplest such interacting system. In particular we will focus on identifying equations governing the critical phase transition in $d = 3$ dimensions both for its expected simplification due to universality and paradoxically for the lack of closed-form exact classification of the limiting behavior of physical observables in its vicinity.

We also formulate a complete basis of nonlinear functions to represent φ^4 theory and explore a strongly coupled fixed point identified using a simple rescaling procedure between these nonlinear functions. We explore the RG equations generated by this technique and produce a set of exponents for this new fixed point.

This thesis is organized as follows: In Chapter 2 we introduce the classical φ^4 action and discuss its known phase transition structure as well as the difficulties in calculating exact analytic results. In Chapter 3 we identify a complete nonlinear basis of functions and use it along with a rescaling approximation to identify and characterize a possible new fixed point. In Chapter 4 we formulate an analytic method to generate RG equations using the Wilsonian-style sharp momentum cutoff nonperturbatively and subsequently use this method on a reduced φ^4-type theory. A proof that the set of nonlinear Jacobi elliptic functions used in Chapter 3 forms a complete basis is given in appendix A.

Chapter 2

Classical φ^4 RG Theory

2.1 The Model

For the following derivation we make use of the particularly clear notes in [36]. From a statistical mechanical perspective we derive the partition function for continuum φ^4 theory in d dimensions from the Ising model on a lattice with lattice spacing a as

$$\mathcal{Z} = \sum_{\{S_i=\pm 1\}} e^{-\mathcal{H}_{\text{Ising}}}. \tag{2.1}$$

The Hamiltonian $\mathcal{H}_{\text{Ising}}$ reads

$$\mathcal{H}_{\text{Ising}} = -\frac{1}{2}\sum_{i,j=1}^{N} K_{ij} S_i S_j, \tag{2.2}$$

where N is the total number of sites on the lattice,

$$K_{ij} = \begin{cases} \beta J & \text{for nearest neighbors } i \text{ and } j \\ 0 & \text{otherwise,} \end{cases} \tag{2.3}$$

$\beta = 1/kT$, and J is the interaction strength between spins with $J > 0$ here. Performing a Hubbard-Stratonovich (HS) transformation

$$\exp\Big(\frac{1}{2}\sum_{ij} K_{ij} S_i S_j\Big) = \sqrt{\frac{\text{detK}}{(2\pi)^N}} \prod_{k=1}^{N} \int_{-\infty}^{\infty} d\theta_k \exp\Big(-\frac{1}{2}\sum_{ij}\theta_i K_{ij}\theta_j + \sum_{ij} S_i K_{ij}\theta_j\Big), \tag{2.4}$$

where K is a matrix formed by elements from Eq.(2.3). The important effect of this transformation is that the spin variables S_i are decoupled, and thus the sum over their values in the partition function Eq.(2.1) can be performed explicitly for the last term term in Eq.(2.4) as

$$\sum_{S_i=\pm 1} \exp\Big(\sum_{ij} S_i K_{ij}\theta_j\Big) = 2^N \prod_i \cosh\Big(\sum_j K_{ij}\theta_j\Big) \tag{2.5}$$

$$= 2^N \exp\Big\{\sum_i \ln\Big[\cosh\Big(\sum_j K_{ij}\theta_j\Big)\Big]\Big\} \tag{2.6}$$

resulting in

$$\mathcal{Z} = \sqrt{\frac{\det \mathrm{K}}{(\frac{\pi}{2})^N}} \prod_{k=1}^{N} \int_{-\infty}^{\infty} d\theta_k \exp\Big\{-\frac{1}{2}\sum_{ij}\theta_i K_{ij}\theta_j + \sum_i \ln\Big[\cosh\Big(\sum_j K_{ij}\theta_j\Big)\Big]\Big\} \tag{2.7}$$

for the partition function. These new degrees of freedom θ_i are continuous and will help us formulate a continuum model for the Ising system.

We can simplify the term $\sum_j K_{ij}\theta_j$ since K_{ij} is a constant K for nearest neighbors and zero otherwise giving

$$\sum_j K_{ij}\theta_j = K \sum_n \theta_{\mathbf{i}+\mathbf{a}_n}, \tag{2.8}$$

where $\mathbf{i} = (i_1, \ldots, i_d)$ is a vector of integers denoting the lattice sites and $\mathbf{a}_n$ are vectors denoting the nearest neighbor directions of which there are $\sum_n$. We can take the continuum limit of the result in Eq.(2.8) as

$$\theta_{\mathbf{i}+\mathbf{a}_n} \to \theta(\mathbf{x}+\mathbf{a}_n) = \theta(\mathbf{x}) + \sum_\alpha \frac{\partial\theta}{\partial x_\alpha} a_{n,\alpha} + \frac{1}{2}\sum_{\alpha,\beta} \frac{\partial^2\theta}{\partial x_\alpha \partial x_\beta} a_{n,\alpha} a_{n,\beta} + \cdots, \tag{2.9}$$

where the indices α and β sum over vector components of the nearest neighbors. The sums given in Eq.(2.9), however, can be reduced in a regular lattice. For example, in a hypercubic lattice we find

$$\sum_n a_{n,\alpha} = 0 \tag{2.10}$$

$$\sum_n a_{n,\alpha} a_{n,\beta} = 2a^2 \delta_{\alpha,\beta} \tag{2.11}$$

, where a is the lattice spacing and δ is the Kronecker delta. This simplifies Eq.(2.8) to

$$K \sum_n \theta_{\mathbf{i}+\mathbf{a}_n} \to Kz\theta(\mathbf{x}) + Ka^2\nabla^2\theta(\mathbf{x}) + \cdots, \tag{2.12}$$

where z is the coordination number of the lattice, e.g. $z = 2d$ for the hypercubic lattice, and ∇^2 is the Laplacian.

We can further expand the last term in Eq.(2.7) using

$$\ln(\cosh(x)) = \frac{x^2}{2} - \frac{x^4}{12} + \cdots , \tag{2.13}$$

where $x = \sum_j K_{ij}\theta_j$ is our simplified quantity in Eq.(2.12). Keeping quadratic terms to $\mathcal{O}(\nabla^2)$ and the quartic term independent of ∇ we obtain for the partition function

$$\mathcal{Z} = \sqrt{\frac{\mathrm{detK}}{(\frac{\pi}{2})^N}} \int \mathrm{D}[\theta(\mathbf{x})] \exp\Big\{ - \int d^d x \Big[\tilde{r}\theta^2(\mathbf{x}) - D\theta(\mathbf{x})\nabla^2\theta(\mathbf{x}) + \tilde{g}\theta^4(\mathbf{x}) + \cdots \Big] \Big\}, \tag{2.14}$$

where we have replaced the N variable integration measure $\prod_k d\theta_k$ with its functional integral limit $D[\theta(\mathbf{x})]$ and we have also defined the coupling constants as

$$\begin{aligned} D &= -\frac{1}{2} K a^2 (1 - 2Kz) && (2.15) \\ \tilde{r} &= \frac{1}{2} Kz(1 - Kz) && (2.16) \\ \tilde{g} &= \frac{1}{12}(Kz)^4. && (2.17) \end{aligned}$$

If we now let

$$D\theta^2(\mathbf{x}) \equiv \varphi^2(\mathbf{x}) \tag{2.18}$$

and redefine the coupling constants as

$$\begin{aligned} r &\equiv \frac{\tilde{r}}{D} = \frac{z(1 - Kz)}{a^2(2Kz - 1)} && (2.19) \\ g &\equiv \frac{\tilde{g}}{D^2} = \frac{(Kz)^4}{3K^2 a^4 (2Kz - 1)^2} && (2.20) \end{aligned}$$

then we obtain the φ^4 action we are seeking

$$\begin{aligned} \mathrm{S} &= \int d^d x \Big(- \varphi(\mathbf{x})\nabla^2\varphi(\mathbf{x}) + r\varphi^2(\mathbf{x}) + g\varphi^4(\mathbf{x}) \Big) && (2.21) \\ \mathrm{S} &= \int d^d x \Big((\nabla\varphi(\mathbf{x}))^2 + r\varphi^2(\mathbf{x}) + g\varphi^4(\mathbf{x}) \Big), && (2.22) \end{aligned}$$

where we have performed an integration by parts in the last line assuming suitable boundary conditions. Finally, the transformation in Eq.(2.18) also introduces a factor of $D^{-N/2}$ in the partition function giving

$$\mathcal{Z} = \sqrt{\frac{\mathrm{detK}}{(\frac{D\pi}{2})^N}} \int D[\varphi(\mathbf{x}] e^{-\mathrm{S}} \tag{2.23}$$

with S given by Eq.(2.22).

It is instructive to analyze the coefficients r and g of φ^4 theory in the vicinity of the true critical point as opposed to the mean field estimate of such a point. Let the critical transition temperature be given in general by T^* and thus $K^* = J/kT^*$. Define the reduced temperature via

$$t \equiv \frac{T - T^*}{T^*} \tag{2.24}$$

so that the transition happens at $t = 0$ for dimensionless t. Then for r and g very close to the transition point $t \ll 1$ and we can rewrite Eqs.(2.19,2.20) as

$$r - r^* = \frac{K^* z^2}{a^2(2K^* z - 1)^2} t + \mathcal{O}(t^2) \tag{2.25}$$

$$g - g^* = \frac{(K^* z^2)^2}{3a^4(2K^* z - 1)} t + \mathcal{O}(t^2), \tag{2.26}$$

where r^* and g^* are the values of the coefficients at the transition. This result shows that $r - r^*$ and $g - g^*$ are proportional to the temperature near a critical point, a fact we will use to our advantage later.

This connection to the Ising model does more than identify φ^4 theory as governing the behavior of magnetic systems, it also shows that the phase transition structure of the continuum theory could very well go beyond that of the Ising model. We can see this by looking at r and g in Eqs.(2.19,2.20). A mean field treatment gives $K^* z = 1$ and thus $r = 0$ as the point where the transition occurs, but the results from mean field theory do not agree with experiments or results from numerical methods. More general theoretical treatments, for example the ϵ-expansion mentioned below, show that the critical point in $d = 3$ is pushed to $r < 0$ by the interactions encoded in the coupling term g. Therefore if a fixed point is found for $r = 0$ and $g \to \infty$ then this point cannot be the Ising critical point. We will later identify and characterize a possible new fixed point for φ^4 theory in Chapter 3 in the limit as $(r, g) \to (0, \infty)$ with behavior in $d = 3$ unlike that found in the Ising model.

Returning to the continuum model, it is more convenient to work in momentum space so we take the Fourier transform of the field

$$\varphi(\mathbf{x}) = \frac{1}{V}\sum_{\mathbf{p}} \varphi_{\mathbf{p}} e^{\mathbf{p}\cdot\mathbf{x}}, \tag{2.27}$$

where the variables $\mathbf{x}$ and $\mathbf{p}$ are assumed to be d-dimensional vectors. We then apply this transform to the action S and integrate over space variables $\mathbf{x}$ to obtain

$$\mathrm{S} = \sum_{\mathbf{p}} (p^2 + r)\varphi_{\mathbf{p}}\varphi_{-\mathbf{p}} + g\frac{1}{V^4}\sum_{\mathbf{p_1},\mathbf{p_2},\mathbf{p_3},\mathbf{p_4}} \delta(\mathbf{p_1}+\mathbf{p_2}+\mathbf{p_3}+\mathbf{p_4})\varphi_{\mathbf{p_1}}\varphi_{\mathbf{p_2}}\varphi_{\mathbf{p_3}}\varphi_{\mathbf{p_4}}, \tag{2.28}$$

where the quadratic part of the action has now been made particularly simple but at the cost of a complicated mixing between momentum states in the quartic term due to the requirement of translational invariance. This work will solve for physical observables subject to Eq.(2.28), which are given by averaging over the partition function

$$< A >= \frac{\int D[\varphi(\mathbf{x})] A e^{-S}}{Z_0}, \tag{2.29}$$

where Z_0 is the partition function from Eq.(2.23). This averaging will help avoid divergences in the integrals due to the arbitrarily large number of variables, but the values those variables take can still diverge for the model given here. In order to deal with these divergences we must introduce constraints on the fields and/or boundary conditions. In this chapter we will review the standard techniques for calculating critical exponents, which take the continuum limit such that the sum over momenta $\mathbf{p}$ becomes an integral and the boundary condition merely requires the field $\varphi(\mathbf{x})$ to be well-behaved at infinity. The two new techniques outlined in the following chapters, however, utilize periodic boundary conditions in real space. We will look at boundary conditions on a d-torus and require the fields to be smooth and finite everywhere.

2.2 The Renormalization Group

We will closely follow Wilson's original description of the Renormalization Group (RG) applied to critical phase transitions. One of the hallmarks of a critical phase transition is that the correlations diverge and many physical observables along with them. In a finite statistical mechanical system each state in the sum, for example any particular configuration of spins in Eq.2.2, gives an analytic contribution to the partition function, and it is only in the infinite thermodynamic limit that such singular behavior occurs in theory [39]. This singular behavior is the source of the difficulties when attempting to work with the partition function as a whole directly in the vicinity of the critical point. The renormalization group (RG) is designed to extract the information contained in a partition function under such circumstances, and it relies on the

vast simplification and ultimate reduction in the number of independent degrees of freedom that dominate the macroscopic properties of a system near a fixed point such as the critical point. However, the general prescription outlined by RG leaves many choices to the researcher regarding its implementation.

In its most general form, RG can be broken down into three steps. First, regularize the action to ensure that all terms are analytic and choose a subset of the remaining degrees of freedom to eliminate. Second, perform the integration outlined in step one and then absorb the result into the remaining original action. Finally, perform a rescaling such that the remaining reduces set of degrees of freedom span the original range chosen in step one. This procedure results in a set of RG equations governing the flow of the coefficients of the theory under coarse-graining that can then be used to identify the fixed points towards which the model flows when the RG process is iterated. Since a statistical mechanical model is fundamentally a microscopic one and thermodynamic observables give macroscopic information, in theory this step-by-step iteration fully characterizes all possible macroscopic states of the model with one major caveat.

Wilson's own largest contribution to this process is that there are constraints that must be upheld throughout the procedure as well. Namely that the action must allow for the inclusion and generation of all possible terms that obey an a priori determined set of symmetries. Without this crucial constraint it is impossible to properly characterize any identified fixed point since the stability or instability of the flow near a particular fixed point identifies it as a bulk phase, discontinuous phase transition, critical point, multicritical point, and so on.

At each stage of the RG process there are many seemingly ad hoc choices left to be made: the set of symmetries governing the action, the type of degrees of freedom to work with, the regularization of those degrees of freedom, the splitting of the degrees of freedom into integrated and remaining sets, and all of this in such a way as to leave the system amenable to a single-parameter rescaling procedure (in the simplest and most common case). In addition to these necessary but somewhat arbitrary choices, the integration step is typically extremely difficult and often involves additional ad hoc assumptions that are not mandated by the renormalization group theory.

Given this plethora of arbitrary choices and the difficulty surrounding the practical integration of a subset of the degrees of freedom in general, it is no wonder that analytic work for continuum field theories has evolved around the rich history of perturbative methods as well as the numerical techniques that Wilson had originally envisioned [41] and worked towards once RG was well-established. Although we will review this rich history briefly below, the focus on this work is on two RG methods developed primarily to handle the integration step in an analytic and nonperturbative way without piling on additional restrictive assumptions. As per the RG formalism we must first choose our degrees of freedom and then regularize the action, but there

are many disparate ways to implement this step. Callan-Symanzyk equations [6, 35] are less intuitive since they regularize the coefficients of the theory at a set energy scale, but they are designed with perturbative calculations in mind and offer little in the way of simplification for our nonperturbative goals. Wilson-Polchinsky exact RG uses a smooth but all-inclusive momentum cutoff and effectively integrates out only part of each momentum in the RG process. This method is very effective for numerical techniques, but it is not amenable to analytic calculations for arbitrary interacting systems as it requires solving an infinite dimensional space of couplings, see e.g. [16]. Real-space lattice methods typically employ the integration of a sublattice of points, but again there is no systematic way to achieve analytic nonperturbative results for strongly coupled theories with this method. Regardless of the specific regularization method employed, the vast majority of degrees of freedom employed for the integration step and thus regularized are momentum or momentum-like (e.g. real-space lattice subspaces rather than single sites are integrated). The justification for this seemingly universal choice is that in the vicinity of fixed points, and critical points specifically, very few degrees of freedom govern the macroscopic system properties and these degrees of freedom are macroscopic themselves. In other words they are Wilson's own original regularization choice was a sharp cutoff in momentum space and we will use it with impunity throughout this work.

Upon choosing the degrees of freedom, restricting their ranges, splitting them into 'slow' and 'fast' modes, and performing an integration step to eliminate the fast modes to thereby modify the remaining slow modes, the Wilsonian RG procedure requires that we rescale the remaining degrees of freedom to regain the original partition function with any changes being absorbed into the coefficients of the action. This is most often done with a single rescaling parameter, and in the case of φ^4 theory discussed here it will be a rescaling of the magnitude of the momentum. There are interesting cases where more than one rescaling parameter is needed [30], but a discussion of such systems is outside the scope of this work.

The culmination of the RG procedure is a set of RG equations determining the change of the coefficients in the action upon implementing this coarse-graining step. This change can be considered as a 'flow' of the action under the coarse-graining, and a common physical picture is that one is zooming out from an initial microscopic system to the ultimate macroscopic system. These RG equations take the form of finite difference equations in the discrete case and differential equations in the continuous case. At this point the RG procedure itself is completed and from this point on the calculation becomes nothing more than an analysis of a coupled set of first order differential equations.

However in large part the original motivation for Wilson's RG theory was to understand phase transitions in general and critical phenomena specifically. Phase transitions and bulk phases have an exceptionally transparent physical interpretation in terms of the equations generated by the RG process. Both phase

transitions and bulk phases are descriptions of thermodynamic systems where the system as a whole takes on single values for state variables. Once one has reached a macroscopic description of a system, changing the scale at which one views that system cannot affect any of its intrinsic properties. In terms of the coefficients of the model governing that system, a change of scale cannot alter the model in any way. Since the RG procedure affects such a change of scale where the only quantities in the model allowed to change with this change of scale are the coefficients of the model, any macroscopic state such as a bulk phase or a phase transition *must* also not allow these coefficients to change. This exactly corresponds to those values of the coefficients where the RG equations do not cause the coefficients to flow; the fixed points of the RG equations identify the phases and phase transitions of the model.

Historically much emphasis has been put on the critical points identified and/or characterized by the RG and this is in part due to the difficulties in understanding critical phase transitions prior to RG and in part due to the fact that many of the other fixed points such as bulk phases often have analytic free energy densities and are thus amenable to more traditional techniques. Yet, discontinuous phase transitions and more complicated transitions such as the BKT transition [22] can often be difficult to identify and characterize as well. In Chapter 3 we will identify a potential previously unknown fixed point with discontinuous character in the $d = 3$ φ^4 theory.

Once all or at least some of the fixed points of the RG equations have been identified, chacterization of each point proceeds independently from the others. The general analysis, as given in section 9.3 of [15], is the same for each point. First one must calculate whether the correlations vanish or diverge. That these are the only two options can be shown in the following way. Suppose we have identified the RG transformation equations

$$K' = R_b[K], \tag{2.30}$$

where K denotes the set of coefficients for a particular model and K' the change in those coefficients after applying a coarse-graining procedure and subsequently rescaling the momentum degrees of freedom by a factor $b \geq 1$. Then any fixed point in coefficient space, denoted by K^*, must satisfy

$$R_b[K^*] = K^*. \tag{2.31}$$

The rescaling factor b implies that all lengths have been rescaled by a factor b^{-1} and in particular the correlation length ξ must transform in general as

$$\xi[K'] = b^{-1}\xi[K], \tag{2.32}$$

where K' indicates the values of the coefficients in the theory after an iteration of the RG procedure. Putting Eq.2.31 and Eq.2.32 together we find that at any fixed point the correlation length must satisfy

$$\xi[K^*] = b^{-1}\xi[K^*] \tag{2.33}$$

The only solutions of which are $\xi = 0$ or $\xi \to \infty$.

As it will come up in the evaluation of the RG equations in Chapter 3, it is worth noting that when the RG equation for a coefficient only contains an arbitrary multiplicative factor of b and no additive terms on the RHS as ξ does in Eq.(2.32) then the *only* allowed fixed point solutions occur at the extreme values for that parameter. In this case $-\xi$ has no physical meaning, so the extreme values are at zero and positive infinity. The extreme value of the correlations dominate the scales of the system and thus the behavior of all of the physics observables: they all tend towards vanishing or diverging values in the vicinity of fixed points. Therefore linearization of the RG equations arbitrarily close to a given fixed point will both simplify the coupled RG equations as well as extract the leading order behavior of the physical observables at that fixed point.

Due to the well-known tendency for power-law behavior to dominate the physical observables at a critical point we expect this behavior in general at a corresponding fixed point. The eigenvalues generated by the above linearization procedure can be used to directly calculate the leading order divergence or vanishing of physical observables as the system approaches a fixed point in the form of the exponents identifying this power-law behavior. It is these exponents that we ultimately seek as they tell us what type of fixed point we have and they indicate any interesting physics at that point.

To calculate these exponents, suppose we are near a fixed point such that

$$K_i = K_i^* + \delta K_i, \tag{2.34}$$

where i enumerates all possible coefficients in the action. Then plugging Eq.(2.34) into Eq.(2.31) and expanding to linear order in δK_i we find that

$$K_i' = K_i^* + \sum_j \delta K_j \frac{\partial K_i'}{\partial K_j}\Big|_{K_j = K_j^*}, \tag{2.35}$$

which generates a linear transformation matrix governing the flow near the fixed point given by

$$M_{ij} = \frac{\partial K_i'}{\partial K_j}\Big|_{K_j = K_j^*}. \tag{2.36}$$

Solving the eigensystem for this transformation matrix $\mathcal{M}$ gives us a set of eigenvalues and eigenvectors which in turn characterize the fixed point completely as follows. In general we can order the eigenvalues by their magnitudes

$$|\Lambda_1| \geq |\Lambda_2| \geq |\Lambda_3| \cdots, \tag{2.37}$$

but how do we relate these eigenvalues to physical observables? The following analysis can be found in e.g. section 9.4.1 of [15].

Suppose that we know the RG transformation for the temperature to be

$$T' = R_b(T), \tag{2.38}$$

where $b > 1$ is the rescaling factor as before. Then linearizing near a fixed point we find

$$T' - T^* = \Lambda_b(T - T^*) + \mathcal{O}((T - T^*)^2), \tag{2.39}$$

where T^* is the fixed point temperature and Λ_b is the eigenvalue of the linearized equation given by

$$\Lambda_b \equiv \frac{\partial R_b}{\partial T}\Big|_{T=T^*}. \tag{2.40}$$

Since the RG equation R_b is defined by a scale change of b, two successive applications of R_b, even for different values b and b', should be equivalent to one scale change bb' giving

$$R_b R_{b'} = R_{bb'}. \tag{2.41}$$

In the case of our linearized equations given by Eq.(2.39) application of Eq.(2.41) results in

$$\Lambda_b \Lambda_{b'} = \Lambda_{bb'} \tag{2.42}$$

$$\Rightarrow \Lambda_b = b^{y_t}, \tag{2.43}$$

where the scaling exponent of the reduced temperature t, given by y_t, is determined via Eq.(2.40). In terms of the reduced temperature, defined in Eq.(2.24) we find

$$t' = tb^{y_t}. \tag{2.44}$$

In order to connect this result to experimental observables, we proceed with a static scaling hypothesis argument. The origins of static scaling are traced back to [38] and the argument presented below continues to follow that of [15]. We can apply the transformation given in Eq.(2.44) an arbitrary number of times n to obtain

$$t^{(n)} = (b^{y_t})^n t. \tag{2.45}$$

The correlation length, on the other hand, scales as b^{-1} as in Eq.(2.32), so n iterations of the RG result in

$$\begin{aligned} \xi(t) &= b^n \xi(t^{(n)}) && (2.46) \\ &= b^n \xi((b^n)^{y_t} t). && (2.47) \end{aligned}$$

The motivation behind choosing arbitrary number n of transformations for arbitrary rescaling factor b is that we are free to choose any value we like for b^n, such as

$$b^n = (\frac{M}{t})^{1/y_t}, \tag{2.48}$$

where is M is an arbitrary large number. This simplifies Eq.(2.47) to give

$$\xi(t) = (\frac{t}{M})^{-1/y_t} \text{ as } \xi(M)t \to 0. \tag{2.49}$$

The exponent ν is defined as $\xi \propto t^{-\nu}$ in the vicinity of a fixed point giving

$$\nu \equiv 1/y_t. \tag{2.50}$$

This gives us one of the two necessary exponents to identify all others at a fixed point.

Recalling from Eqs.(2.25,2.26) $r - r^*, g - g^* \propto t$ near a critical point in φ^4 theory. In general the largest eigenvalue of a linearized set of equations such as in Eq.(2.35) dominates the behavior of that system in the limit of a large number of iterations. In other words if we are close enough to the critical point then we can

apply enough iterations of the linearized RG equations such that the behavior is governed by the largest eigenvalue alone, which is given by Λ_1 from Eq.(2.37). However by definition the linearized RG equations are controlled by the reduced temperature t. Therefore when we linearize the RG equations for r and g and identify eigenvalues of that system, then the largest one $|\Lambda_1| = y_t$ and thus gives ν via Eq.(2.50). The other exponent we will find, the anomalous dimension η, is defined as the scaling of the field near the fixed point denoted

$$\varphi'_k = Z\varphi_k \equiv b^{(d-2+\eta)/2}\varphi_k \tag{2.51}$$

as given in e.g. section 13.1 of [29], where $b > 1$ is the rescaling factor required to ensure that the remaining degrees of freedom after coarse-graining span the original range. Solving for η we find that

$$\eta = 2 - d + 2\frac{\mathrm{lnZ}^*}{\mathrm{lnb}}, \tag{2.52}$$

where Z^* is the field rescaling factor at the critical point. These two exponents are all that we need in order to calculate the remaining ones through the use of scaling laws, and they will be the focus of our efforts.
Besides using the eigenvalues of the linear transformation near a fixed point to directly read off these universal exponents, the eigenvalues taken together can also characterize the type of macroscopic state that the fixed point represents. Eigenvalues that are greater, equal to, or less than unity are characterized as relevant, marginal, and irrelevant respectively, and the number of relevant directions identifies the state. For example, if there are no relevant directions then the fixed point identifies a bulk phase, whereas a critical point needs at least two relevant directions. The number of relevant directions does not uniquely define a state, however, as a triple point also has two relevant directions. In addition to finding the number of relevant directions, calculating the correlation length will settle this issue as only critical phenomena have diverging correlations whereas discontinuous phase transitions and bulk phases are characterized by a finite correlation length. Finally, it is important to emphasize that this procedure must be done at each fixed point independently of the others as the macroscopic nature of the system is typically vastly different at each phase transition vs one or another bulk phase.
As a helpful reference we include the most commonly calculated physical observables for phase transitions and their corresponding variables in Table 2.1.

Since identification of any two exponents generates the remaining ones through the application of scaling laws, we provide a list of the most common ones for quick reference in Table 2.2.

If any such exponent should be zero, then the next highest leading order corrections, typically logarithmic

Table 2.1: Several common physical observable exponent conventions.

Observable	Exponent Variable
Correlation Length	ν
Anomalous Dimension	η
Heat Capacity	α
Spontaneous Magnetization	β
Susceptibility	γ
Order Parameter	δ

Table 2.2: Scaling relations among several common exponents.

Scaling Law	Relation
Josephson	$2 - \alpha = \nu d$
Griffiths	$\beta\delta = \beta + \gamma$
Rushbrooke	$\alpha + 2\beta + \gamma = 2$
Fisher	$\nu(2 - \eta) = \gamma$

divergences, are sought after. These logarithmic divergences obey their own version of scaling relations as given in [20].

One of the most powerful and natural consequences of RG theory is the principle of universality, or the tendency for many seemingly disparate microscopic models to give rise to the same macroscopic behavior. The RG equation flow analysis provides a particularly clear picture of this effect in that there are typically very few points in coefficient space that are fixed points, and yet the remaining vast majority of points, each corresponding to a different microscopic system, must ultimately flow to one of these few points. This maps domains of the 'space of microscopic theories' for a given model to the same single macroscopic state. This statement can be turned around to argue that the discovery of a general procedure to generate analytic nonperturbative RG equations and thus identify all fixed points and the values of physical observables near those points for even one model is highly likely to have far reaching consequences since the principle of universality indicates that these exact solutions should hold for many seemingly different systems. Hence the principle of universality lends further intrinsic value to such a pursuit.

2.3 Landau Mean Field Critical Theory

Before delving into the Renormalization Group theory further, a mean field analysis for φ^4 theory will help put the problem into perspective. In a Landau-style mean field treatment, e.g. see section 5.7 of [15], we add a term linear in φ to Eq.(2.21) representing the interactions with an external field as

$$\mathcal{L} = \int d^d x \Big(-\varphi(\mathbf{x})\nabla^2\varphi(\mathbf{x}) + r\varphi^2(\mathbf{x}) + g\varphi^4(\mathbf{x}) + h(\mathbf{x})\varphi(\mathbf{x}) \Big). \tag{2.53}$$

We can set $h = 0$ at the end of any thermodymanic calculation, for example, to determine the zero-field values, but introducing the external field is useful for performing the calculations below.

We first calculate the two-point correlation function by minimizing $\mathcal{L}$ with respect to $\varphi(\mathbf{x})$ as

$$\frac{\delta \mathcal{L}}{\delta \varphi(\mathbf{x})} = 0 = \nabla^2 \varphi(\mathbf{x}) + r\varphi(\mathbf{x}) + 4g\varphi^3(\mathbf{x}) - h(\mathbf{x}) \tag{2.54}$$

and then differentiating with respect to $h(\mathbf{x})$ to find the equation for the susceptibility χ

$$\Big(-\nabla^2 + 2r + 12g\varphi^2(\mathbf{x})\Big)\chi(\mathbf{x}, \mathbf{x}') = \delta(\mathbf{x} - \mathbf{x}'). \tag{2.55}$$

Now according to the static susceptibility sum rule, see e.g. section 3.7.2 in [15], the two-point correlation function is proportional to the susceptibility via

$$G(\mathbf{x} - \mathbf{x}') = k_B T \chi(\mathbf{x} - \mathbf{x}'), \tag{2.56}$$

where we have used the fact that the system is translationally invariant to let $\mathbf{x}, \mathbf{x}' \to \mathbf{x} - \mathbf{x}'$. Thus the equation governing the correlation function is

$$\Big(-\nabla^2 + 2r + 12g\varphi^2(\mathbf{x})\Big) G(\mathbf{x} - \mathbf{x}') = k_B T \delta(\mathbf{x} - \mathbf{x}'). \tag{2.57}$$

The definition of ν is the scaling exponent of the correlation length near the critical transition. In this mean field analysis the order parameter is simply the equilibrium value of $\varphi(\mathbf{x})$ assuming a translationally invariant system. In order to find this value we minimize Eq.(2.54) setting $h = 0$ and assuming φ is a constant independent of $\mathbf{x}$ resulting in

$$0 = 2r\varphi + 12g\varphi^3. \tag{2.58}$$

There are two solutions depending on the sign of r. Recalling that $r \propto t = (T - T^*)/T^*$ we find

$$\varphi = \begin{cases} 0 & T \geq T^* \\ \sqrt{\frac{-r}{6g}} & T < T^*, \end{cases} \tag{2.59}$$

which shows that the system undergoes an ordering phase transition at the mean field level as r passes through zero.

The definition of the correlation length is the characteristic fall-off of the correlations with distance. In this

case Eq.(2.57) for constant φ defines the correlation length to be

$$\xi^{-2} \equiv 2r + 12g\varphi^2 \tag{2.60}$$

Rewriting Eq.(2.57) to include the definition of the correlation length in Eq.(2.60) we find that

$$\Big(-\nabla^2 + \xi^{-2}\Big) G(\mathbf{x} - \mathbf{x}') = k_B T \delta(\mathbf{x} - \mathbf{x}'). \tag{2.61}$$

Further taking the Fourier transform of this equation results in

$$\tilde{G}(\mathbf{k}) = k_b T \frac{1}{k^2 + \xi^{-2}}, \tag{2.62}$$

where plugging Eq.(2.59) into gives $\xi = \sqrt{1/2r}$ for $r \geq 0$ and $\xi = \sqrt{-1/4r}$ for $r < 0$. In either case we find that since $r \propto t$ the value of the correlation length near the transition becomes

$$\xi(t) \propto t^{-1/2}. \tag{2.63}$$

By the definition of the correlation length exponent $\xi(t) \propto t^{-\nu}$ we find

$$\nu = \frac{1}{2}. \tag{2.64}$$

In order to obtain the anomalous dimension η we note that as $T \to T^*$ the correlations diverge and thus $\xi^{-2} \to 0$ reducing Eq.(2.62) to

$$\tilde{G}(\mathbf{k}) \to k_B T k^{-2}. \tag{2.65}$$

The anomalous dimension is defined as the deviation of the correlation function from k^{-2} behavior at T^* thus we find

$$\eta = 0, \tag{2.66}$$

and the rest of the exponents follow from the scaling laws. A list of these exponents is given in Table 2.3 below alongside the results from the next section for comparison.

2.4 Exact Results in $d = 2$

Historically much of the motivation behind understanding critical behavior on a theoretical level can be traced back to the exact solution of the Ising model in $d = 2$ dimensions by Onsager [28]. These exact exponents for a nontrivial critical phase transition not only led to a much better understanding of the underpinnings of critical phenomena but also provided a benchmark for testing new methods against. We briefly review Onsager's results here. The central result of Onsager's work on the $d = 2$ Ising model is an exact expression for the partition function. On a square lattice as in section 12.3 of [29] this is given by

$$\frac{1}{N}\ln\mathcal{Z}(\mathrm{T}) = \ln[2^{1/2}\cosh(2\mathrm{K})] + \frac{1}{\pi}\int_0^{\pi/2} \mathrm{d}\theta \ln[1 + \sqrt{1 - \mathrm{m}\,\sin^2(\theta)}], \tag{2.67}$$

where N is the number of sites. K and m are defined by

$$K = \frac{J}{k_B T} \tag{2.68}$$

$$m = \frac{4\sinh^2(2\mathrm{K})}{\cosh^4(2\mathrm{K})}, \tag{2.69}$$

where J is the Ising interaction strength and T is the temperature. If one is fortunate enough to have an exact expression for the partition function, then analytic calculation of physical observables is a very straightforward exercise in statistical mechanics. From our discussion in the previous section we are most interested in quantities arbitrarily close to the critical phase transition point and since these diverge there we expect power-law leading order behavior.

To calculate the specific heat, for example, we differentiate Eq.(2.67) with respect to $-\beta = 1/k_B T$ followed by differentiation with respect to temperature T. This results in an exact expression for the dimensionless specific heat

$$\frac{C_0(T)}{N k_B} = \frac{2}{\pi} K^2 \coth^2(2\mathrm{K})\{2(\mathrm{K}_1(\mathrm{m}) - \mathrm{E}_1(\mathrm{m})) - (1 - \sqrt{1 - \mathrm{m}})(\frac{\pi}{2} + \sqrt{1 - \mathrm{m}}\mathrm{K}_1(\mathrm{m}))\}, \tag{2.70}$$

where $K_1(m)$ and $E_1(m)$ are the complete elliptic integrals of the first and second kind respectively. As $m \to 1$ $K_1(m) \to \ln(4/\sqrt{\mathrm{m} - 1})$ and $E_1(m) \to 1$ resulting in a logarithmic singularity for the specific heat at the critical temperature, which is given by

$$\sinh(2\mathrm{K_c}) = 1. \tag{2.71}$$

A logarithmic divergence as the leading order behavior near the critical point indicates that the exponent for power-law behavior vanishes, thus $\alpha = 0$. Using the eigenvalues of a transfer matrix method, a calculation for the correlation length exponent results in $\nu = 1$,see e.g. [5], and from these two exponents we can use scaling laws to determine the remaining exponents of interest given in Table 2.3. We include the results for the mean field exponents alongside those of Onsager to show just how different these two phase transitions are. In particular the correlations are much stronger in the Onsager case than in mean field. Although $\alpha = 0$ for both transitions, the leading order logarithmic corrections are just as different as the leading order power-law behavior for the correlations [20].

Table 2.3: Onsager and Ising Mean Field Critical Exponents

FP	Onsager	Mean Field
ν	1	$\frac{1}{2}$
η	$\frac{1}{4}$	0
α	0	0
β	$\frac{1}{8}$	$\frac{1}{2}$
γ	$\frac{7}{4}$	1
δ	15	3

2.5 Perturbative RG: Wilson-Fisher Fixed Point in $d = 4 - \epsilon$

Given the success of Onsager in treating the critical point of the Ising model exactly in $d = 2$ dimensions and the simplicity of the mean field critical behavior in the same model for $d \geq 4$, one might expect that with time the $d = 3$ critical transition would be solved exactly as well. The earliest systematic analytic treatment of this fixed point came shortly after Wilson developed the renormaliation group in the form of a perturbative expansion near the $d = 4$ mean field system, see for example [43]. We briefly review the results and shortcomings of this method, which represents some of the most ubiquitous analytic techniques in phase transition research.

As outlined in sections 7 and 8 of [43] and detailed in many publications before and since, this method relies on the fact that less than but arbitrarily close to the upper critical dimension $d = 4$ the coupling strength $g \propto \epsilon \equiv 4 - d$. Therefore a Feynman diagram style perturbation series in g is justified. In general if we then calculate the RG equations to a certain order in powers of g and subsequently identify the nontrivial fixed point, then the exponents near that point should give deviations from those of mean field values. This is the case and we list these exponents to $\mathcal{O}(\epsilon^2)$ as well as the slightly dubious but common practice of setting $\epsilon = 1$ to estimate the $d = 3$ critical exponents in Table 2.4. We also include the most recent and highest precision published as of this work in the table. This precision has been obtained using the conformal

bootstrap method [32].

Table 2.4: Wilson-Fisher Critical Exponents to $\mathcal{O}(\epsilon^2)$ and current highest precision calculation of $d = 3$ Ising exponents using the conformal bootstrap method [12].

Exponent	$\mathcal{O}(\epsilon^2)$	$d = 3$ $\epsilon = 1$ Estimate	$d = 3$ Ising
ν	$\frac{1}{2} + \frac{1}{12}\epsilon + \frac{7}{162}\epsilon^2$	0.627	0.629971(4)
η	$\frac{1}{54}\epsilon^2$	0.019	0.036298(2)
α	$\frac{1}{6}\epsilon - \frac{1}{324}\epsilon^2$	0.164	0.11008(1)
β	$\frac{1}{2} - \frac{1}{6}\epsilon + \frac{1}{162}\epsilon^2$	0.340	0.326419(3)
γ	$1 + \frac{1}{6}\epsilon + \frac{1}{972}\epsilon^2$	1.167	1.237075(10)
δ	$3 + \epsilon + \frac{25}{54}\epsilon^2$	4.463	4.78984(1)

The results of this perturbative method are promising, but it turns out that if one goes on to calculate higher and higher order corrections in the series the exponents eventually begin to deviate further and further from those calculated in e.g. the conformal bootstrap method. This illness seems to plague most if not all perturbative methods and is often attributed to either the formal divergence of the series or less accurately to the large value of the perturbation parameter used [34].

This is the state of affairs for the φ^4 analytic work to-date. There are numerical calculations both using large size lattices as well as Wilson-Polchinsky exact RG continuum models that obtain results in agreement with but less precise than those given in the last column of Table 2.4.

Chapter 3

Nonlinear Basis Rescaling and a New Strongly Coupled Fixed Point

It is clear from the previous chapter that perturbative RG vastly improved our ability to understand and predict critical phase transition phenomena, including that of the $d = 3$ magnetic transition present in φ^4 theory. This understanding relies heavily on the momentum-space description of the fields and treats the coupling strength g as small. Although the requirements $g \ll 1$ and $4 - d \ll 1$ are relaxed at the end of the calculation with remarkably good results they still have their limitations. These methods have only been able to calculate the critical exponents to about 2-3 decimal places. Advances in conformal bootstrap methods, see e.g. [32], have increased the precision but are still perturbative in nature.

Calculating fixed point exponents nonperturbatively will require substantial departure from these traditional methods. Much of the material given throughout this chapter is published in [17], however in the course of this work we have identified changes in the resulting exponents, in particular the value of η, which depart from [17] and will require changes to that paper. The publication concerns one such departure from traditional methods that considers altering the microscopic degrees of freedom directly. Momentum states are only eigenstates of a system devoid of interactions, and the primary motivation to use them at all when interactions are nontrivial is to take advantage of the powerful mathematics behind complete linear bases. Provided one can expand the interactions about the free system (hence the requirement that $g \ll 1$), the momentum states reduce the functional integrals to Gaussian integrals that are readily solved.

In order to retain some essence of these powerful techniques while overcoming the need to treat the interaction strength g perturbatively, we will start with the complete linear basis of states and relax just one property: linearity. It is the natural property to relax since strong coupling strength g guarantees that the momentum states are far from eigenvalues. We begin our nonperturbative calculation with this simply stated but nontrivial change to our microscopic state counting.

3.1 Construction of a Complete Nonlinear Basis

Our goal is to encode the interactions in a non-trivial way but still retain a complete representation of the physical system. We will first simplify the action to produce a nonlinear differential equation over the fields. We then solve this equation under periodic boundary conditions and subsequently show that this family of solutions forms a complete basis in d-dimensional space and thus consists of 'all' solutions to this nonlinear differential equation under periodic boundary conditions. We can use integration by parts on the gradient term to separate out one copy of the field

$$\begin{aligned} S &= -\int d^d x \left\{-\varphi(\mathbf{x})\nabla^2\varphi(\mathbf{x}) + r\varphi^2(\mathbf{x}) + g\varphi^4(\mathbf{x})\right\} && (3.1)\\ &= -\int d^d x \varphi(\mathbf{x}) \left\{-\nabla^2\varphi(\mathbf{x}) + r\varphi(\mathbf{x}) + g\varphi^3(\mathbf{x})\right\} && (3.2)\\ &= -\int d^d x \varphi(\mathbf{x}) \mathcal{N}\varphi(\mathbf{x}), && (3.3) \end{aligned}$$

where

$$\mathcal{N} = -\nabla^2 + r + g\varphi^2(\mathbf{x}) \tag{3.4}$$

is a nonlinear operator involving the field φ itself. A simple way to encode the interactions into the degrees of freedom, at least in part, is to solve a reduced nonlinear eigenvalue problem for $\mathcal{N}$

$$\mathcal{N}'\varphi_{\mathbf{n}} = -\nabla^2\varphi_{\mathbf{n}} + r\varphi_{\mathbf{n}} + g\varphi_{\mathbf{n}}^3 = \lambda_{\mathbf{n}}\varphi_{\mathbf{n}} \tag{3.5}$$

where we have neglected mixed cubic terms appearing in the full solution of $\mathcal{N}\varphi_{\mathbf{n}} = \lambda_{\mathbf{n}}\varphi_{\mathbf{n}}$. This reduced equation has a known set of solutions, for $g > 0$, in terms of Jacobi elliptic sine functions

$$\begin{aligned} \varphi_{\mathbf{n}} &= c_{\mathbf{n}}\mathrm{sn}(\mathbf{p}_{\mathbf{n}} \cdot \mathbf{x} + \theta | m_{\mathbf{n}}) && (3.6)\\ \lambda_{\mathbf{n}} &= p_{\mathbf{n}}^2 + r + \frac{g c_{\mathbf{n}}^2}{2} && (3.7)\\ m_{\mathbf{n}} &= \frac{g c_{\mathbf{n}}^2}{2 p_{\mathbf{n}}^2} && (3.8)\\ p_{\mathbf{n}} &= \frac{4K(m_{\mathbf{n}})\mathbf{n}}{L} && (3.9)\\ \mathbf{n} &= (n_1, \ldots, n_d) && (3.10) \end{aligned}$$

where $c_{\mathbf{n}}$ is the amplitude of $\varphi_{\mathbf{n}}$, $K(m)$ is the complete elliptic integral of the first kind given by

$$K(m) = \int_0^1 dt \frac{1}{\sqrt{(1-t^2)(1-mt^2)}}, \tag{3.11}$$

and m is the elliptic modulus. Notice that $p_{\mathbf{n}}$ plays a role similar to that of momentum for a noninteracting system in that only integer multiples of $4K(m)/L$ are allowed due to the periodic boundary. The odd and even solutions are given by $\theta = 0$ and $\theta = K(m)$ respectively. The main goal of this section is to show that despite the loss of orthogonality this set of solutions constitutes a complete but nonlinear basis for any function defined on periodic boundary conditions and thus can be used as the complete set of states describing the partition function.

By complete basis we mean the following. Let a set of real scalar functions $g_n(\mathbf{x})$ be such that an arbitrary real scalar function $f(\mathbf{x})$ can be written as

$$f(\mathbf{x}) = \sum_n a_n g_n(\mathbf{x}), \tag{3.12}$$

where the a_n are also real. If the set of $g_n(\mathbf{x})$ span all possible choices for $f(\mathbf{x})$, then they are said to form a basis. If neglecting any single $g_n(\mathbf{x})$ would result in a set of functions that do not span all choices for $f(\mathbf{x})$, then the set is said to be complete.

Next we describe a few properties of the Jacobi elliptic sine functions. For real bounded functions the elliptic modulus $m \in [0, 1]$ with familiar limiting solutions

$$\lim_{m\to 0} \mathrm{sn}(x|m) \to \sin(x) \tag{3.13}$$

$$\lim_{m\to 0} \mathrm{sn}(x + K(m)|m) \to \cos(x) \tag{3.14}$$

$$\lim_{m\to 1} \mathrm{sn}(x|m) \to \tanh(x) \tag{3.15}$$

$$\lim_{m\to 1} \mathrm{sn}(x + K(m)|m) \to 1. \tag{3.16}$$

Restriction to a periodic boundary L on a d-dimensional torus also further restricts real solutions to $m \in [0, 1)$ and the limiting solutions become

$$\lim_{m\to 0} \mathrm{sn}\left(\frac{4K(m)\mathbf{n}\cdot\mathbf{x}}{L}\Big|m\right) \to \sin\left(\frac{2\pi\mathbf{n}\cdot\mathbf{x}}{L}\right) \tag{3.17}$$

$$\lim_{m\to 0} \mathrm{sn}\left(\frac{4K(m)\mathbf{n}\cdot\mathbf{x}}{L}+K(m)\Big|m\right) \to \cos\left(\frac{2\pi\mathbf{n}\cdot\mathbf{x}}{L}\right) \tag{3.18}$$

$$\lim_{m\to 1} \mathrm{sn}\left(\frac{4K(m)\mathbf{n}\cdot\mathbf{x}}{L}\Big|m\right) \to \mathrm{S}\left(\frac{\mathbf{n}\cdot\mathbf{x}}{L}\right) \tag{3.19}$$

$$\lim_{m\to 1} \mathrm{sn}\left(\frac{4K(m)\mathbf{n}\cdot\mathbf{x}}{L}+K(m)\Big|m\right) \to \mathrm{S}\left(\frac{\mathbf{n}\cdot\mathbf{x}}{L}+\frac{\pi}{2}\right) \tag{3.20}$$

where $\mathbf{n} = (n_1, n_2, \ldots, n_d)$, $n_i \in \mathbb{I}$, and $\mathrm{S}(x)$ is the square wave function given by

$$S(x) = \mathrm{sgn}\Big[\sin(x)\Big]. \tag{3.21}$$

In the Fourier series representation of these functions, e.g. see equation 22.11.1 of [11],

$$\mathrm{sn}\left(\frac{4K(m)\mathbf{n}\cdot\mathbf{x}}{L}\Big|m\right) = \frac{2\pi}{K(m)\sqrt{m}}\sum_{j=0}^{\infty}\frac{q^{j+1/2}}{1-q^{2j+1}}\sin\left(\frac{2\pi(2j+1)\mathbf{n}\cdot\mathbf{x}}{L}\right) \tag{3.22}$$

$$q = \exp\left(-\pi K'(m)/K(m)\right) \tag{3.23}$$

we see that each solution of Eq.(3.5) contains a unique lowest Fourier mode $\sin(2\pi\mathbf{n}\cdot\mathbf{x}/L)$, which also indicates the period of that function. A relatively straightforward proof by induction shows that for each Fourier component of an arbitrary function defined on a periodic boundary the amplitude of the function in Eq.(3.6) with corresponding lowest Fourier mode is uniquely determined. This creates a bijective map from the solutions of Eq.(3.5) to the Fourier basis and completes our proof that these solutions form a complete basis. In fact any set of functions ordered by unique lowest Fourier mode in this way should form a complete basis. Further details of the derivation of this basis and its proof are given in appendix A.

3.2 Separation of the Action as $g \to \infty$

It is well known that at $g = 0$ the action, and thus the partition function, is separable in the Fourier representation. Taking $\varphi(x) = \sum_{\mathbf{n}} a_{\mathbf{n}}\sin(\mathbf{p_n}\cdot\mathbf{x}) + b_{\mathbf{n}}\cos(\mathbf{p_n}\cdot\mathbf{x})$ with $p_{\mathbf{n}} = 2\pi\mathbf{n}/L$ we find

$$\mathcal{Z} = \int \mathcal{D}\{\varphi\}\exp(-S[\varphi]) \tag{3.24}$$

$$= \int \prod_{\mathbf{n}} da_{\mathbf{n}}\ db_{\mathbf{n}} \exp\left\{-L^d \frac{1}{2}\sum_{\mathbf{n}}(\mathbf{p}_n^2 + r)(a_{\mathbf{n}}^2 + b_{\mathbf{n}}^2)\right\} \tag{3.25}$$

$$= \prod_{\mathbf{n}} \int da_{\mathbf{n}}\ db_{\mathbf{n}} \exp\left\{-L^d \frac{1}{2}(\mathbf{p}_{\mathbf{n}}^2 + r)(a_{\mathbf{n}}^2 + b_{\mathbf{n}}^2)\right\} \tag{3.26}$$

and thus the integral over the product of Fourier amplitudes becomes a product over separated integrals. In order to generate RG equations some number of 'fast' modes from the partition function are integrated over. In the case that the action separates, this integration is trivial in that it cannot produce terms that connect the remaining degrees of freedom. In such a situation this integration has no effect on the RG equations and the only contribution comes from rescaling the remaining degrees of freedom to regain those lost by integration. Most of the difficulties in calculating RG equations come from the complications involved in the integration step.

The situation for arbitrary g is not so simple. The representation of the quartic term in a Fourier basis expansion produces complicated mixing between those basis functions. The elliptic basis functions seem to fare no better. Expanding the fields $\varphi(\mathbf{x})$ in terms of the elliptic basis as

$$\varphi(\mathbf{x}) = \sum_{\mathbf{n}} \varphi_{\mathbf{n}}, \tag{3.27}$$

where $\varphi_{\mathbf{n}}$ is given in Eq.(3.6), we find the action to be

$$S = \int d^d x \left\{\sum_{\mathbf{m},\mathbf{n}}(p_{\mathbf{n}}^2 + r)\varphi_{\mathbf{m}}\varphi_{\mathbf{n}} + g \sum_{\mathbf{m},\mathbf{n},\mathbf{o},\mathbf{p}} \varphi_{\mathbf{m}}\varphi_{\mathbf{n}}\varphi_{\mathbf{o}}\varphi_{\mathbf{p}}\right\}. \tag{3.28}$$

At first glance it seems like Eq.(3.28) just further complicates the problem of mixing basis functions since now even the quadratic terms are mixed!

We now make a fairly bold ad hoc assumption: let's keep only the separable part of the action given by

$$\tilde{S} = \sum_{\mathbf{n}} \left\{ \int d^d x \lambda_{\mathbf{n}} c_{\mathbf{n}}^2 \mathrm{sn}^2(p_{\mathbf{n}} \cdot \mathbf{x}|m_{\mathbf{n}})\right\} \tag{3.29}$$

$$= \sum_{\mathbf{n}} \left\{ \int d^d x \left(p_{\mathbf{n}}^2 + r + \frac{g c_{\mathbf{n}}^2}{2}\right) c_{\mathbf{n}}^2 \mathrm{sn}^2(p_{\mathbf{n}} \cdot \mathbf{x}|m_{\mathbf{n}})\right\}. \tag{3.30}$$

Unlike the separable part of the action in the Fourier basis, which is hardly more than the quadratic terms given in Eq.(3.26), the action $\tilde{S}$ includes many interaction terms, although many have also been neglected. There are some properties of the elliptic basis that motivate this simplification. First, the measure is separated despite the fact that the $\varphi_{\mathbf{n}}$ are nonlinear and not completely orthogonal. We can see this by starting with the measure in Fourier space given by

$$\mathcal{D}[\varphi] = \prod_{\mathbf{k}} da_{\mathbf{k}} db_{\mathbf{k}}, \tag{3.31}$$

where we have used the notation for the Fourier series amplitudes as in Eq.(3.26). In order to transform this measure to our elliptic basis amplitudes, we first calculate the determinant of the Jacobian with elements given by

$$\mathrm{J}_{\mathbf{kl}} = \frac{\partial a_{\mathbf{k}}}{\partial c_{\mathbf{l}}} \tag{3.32}$$

where $c_{\mathbf{l}}$ is the amplitude of the elliptic basis function $\varphi_{\mathbf{l}}$ and we are ignoring values of $\theta \neq 0$ in Eq.(3.6) and thus b_n for brevity since the odd functions, given by $\theta = 0$, are by definition orthogonal to the even functions, given by $\theta = K(m)$. Note that $\theta = 0$ basis functions only involve sine functions and we can write in general

$$\varphi_{\mathbf{l}} \equiv \sum_{\mathbf{k}} a_{\mathbf{k}} \sin\Big(\frac{2\pi \mathbf{k}\cdot\mathbf{x}}{L}\Big). \tag{3.33}$$

Using Eq.(3.22) we can thus calculate each element as

$$\mathrm{J}_{\mathbf{kl}} = \begin{cases} \frac{2\pi}{\sqrt{m_1}K(m_1)} \frac{q^{j+1/2}}{1-q^{2j+1}} & \mathbf{k} = (2j+1)\mathbf{l} \\ 0 & \text{otherwise.} \end{cases} \tag{3.34}$$

The important point here is that the index $j \in \{0, 1, \ldots\}$, thus the lowest nonzero term occurs when $\mathbf{k} = \mathbf{l}$. We can in general order the values of $\mathbf{k}$ first by magnitude $|\mathbf{k}|$ and then by, for example, angle from an arbitrarily chosen axis for the degenerate number of $\mathbf{k}$ with the same magnitude. This ordering ensures that the first nonzero element in row $\mathbf{k}$ of the matrix generated by the elements in Eq.(3.34) is when $\mathbf{k} = \mathbf{l}$. Therefore all elements to the left of the diagonal are 0 identically and the matrix is upper triangular. The determinant of a triangular matrix is simply the product of the diagonal elements giving

$$\prod_{\mathbf{k}} dc_{\mathbf{l}} = \det\mathbf{J} \prod_{\mathbf{k}} da_{\mathbf{k}}, \tag{3.35}$$

where

$$\det \mathbf{J} = \prod_{\mathbf{k}} J_{\mathbf{kk}} \tag{3.36}$$

with $J_{\mathbf{kk}}$ given by Eq.(3.34). We are looking for the inverse transformation that starts with $da_{\mathbf{k}}$ and finds the measure for $dc_{\mathbf{l}}$. Since the inverse of a triangular matrix is triangular, the determinant of the inverse transformation is also simply a product of the diagonal elements and is thus separable.

Another motivation for the simplification of the action is that despite the elliptic basis being nonlinear, there are far fewer nonorthogonal basis functions than one might expect at first glance. To see this, we return to the Fourier series representation of the elliptic functions given by Eq.(3.22). Identifying elliptic basis functions that are orthogonal is no more difficult than simply identifying those functions that have mutually independent Fourier series mode expansions. Since the expansion of an elliptic basis functions $\varphi_{\mathbf{n}}$ includes *only* odd powers of a unique lowest Fourier mode with momentum value $\mathbf{k}$ given by

$$\mathbf{k} \equiv \frac{2\pi \mathbf{n}}{L} \tag{3.37}$$

it is clear that the basis functions with index $\mathbf{n}$ along a line intersecting the origin can be nonorthogonal to each other, but are orthogonal to *all* other basis functions! This can be seen by noting that the basis function $\mathbf{n}$ contains only odd *scalar* multiples of $\mathbf{k}$, and thus all Fourier modes in it's expansion lie along this line.

Further, due to the odd scalar multiple restriction mentioned above, most of the basis functions along one such line are also orthogonal to each other! This is due to the Fourier expansion containing only *odd* scalar multiples of the momentum $\mathbf{k}$. In fact such an odd-power expansion groups the nonorthogonal basis functions into sets as follows. Along a given line through the origin , choose an index $\mathbf{n}$ such that $|\mathbf{n}| = 2^m$ for some $m \in \{1, 2, 3, \ldots\}$. Then odd multiples, and *only* odd multiples, of that basis function will be nonorthogonal to it. This forms a set of mutually dependent nonorthogonal functions which are orthogonal to all other such sets. Therefore these basis functions have a high degree of orthogonality despite being inherently nonlinear.

These motivations are not meant to be a formal proof that this simplified action is exact at any point in coupling constant space. A thorough treatment will necessarily require inclusion of the neglected terms at the very least given the possibility that some relevant part of the action has been eliminated by this simplification. Never-the-less we will find that, in the proximity of the Gaussian point as well an as-of-yet unexplored strongly coupled fixed point

$$(r,g) \rightarrow (0,0) \tag{3.38}$$

$$(r,g) \rightarrow (0,\infty) \tag{3.39}$$

respectively, the separable part of the action parameterized by the nonlinear basis given by Eq.(3.7) will identify fixed point solutions. Emphasis should be given at this point that there have been numerous studies on a fixed point at strong coupling in φ^4 theory [4,21], but these studies all require the bare value of $r \rightarrow -\infty$ as $g \rightarrow \infty$. Thus a study about the point $(r,g) \rightarrow (0,\infty)$ is independent of previous studies.

Since the basis functions are ordered by unique lowest Fourier mode, we apply a hyperspherical cutoff in these functions $|\mathbf{n}| \leq |\mathbf{n}_0|$ to Eq.(3.30) and then split these modes into 'fast' and 'slow' sets via a parameter b as follows. Let the lowest Fourier mode of a given basis function $\mathbf{p_n}$ be given by $\mathbf{k_n} = 2\pi\mathbf{n}/L$. Then the slow modes satisfy

$$\mathbf{k}_< \equiv |\mathbf{k_n}| \in [0, \mathbf{k}_{\mathbf{n}_0}/b]$$

and the fast modes satisfy

$$\mathbf{k}_> \equiv |\mathbf{k_n}| \in [\mathbf{k}_{\mathbf{n}_0}/b, k_{\mathbf{n}_0}].$$

Since these lowest Fourier modes are in one-to-one correspondance with the basis functions we can use the same $<,>$ notation for the indices themselves, resulting in

$$S_< = \int d^dx \left(\mathbf{p}_<^2 + r + \frac{gc_<^2}{2}\right) c_<^2 \mathrm{sn}^2(\mathbf{p}_< \cdot \mathbf{x}|m_<) \tag{3.40}$$

$$S_> = \int d^dx \left(\mathbf{p}_>^2 + r + \frac{gc_>^2}{2}\right) c_>^2 \mathrm{sn}^2(\mathbf{p}_> \cdot \mathbf{x}|m_>), \tag{3.41}$$

where $S_{<(>)}$ denotes the part of the separable action containing 'slow'('fast') modes respectively. Since the basis functions are separated in Eq.(3.30), integrating out $S_>$ does not alter $S_<$.

Having truncated the action to the separable form given by Eq.(3.30), we now have to try to obtain some information from it concerning a possible new fixed point. Of course, since in Eq.(3.30) the partition function is simply a product of one-dimensional definite integrals over each of the amplitudes c_n, we could in principle evaluate the latter explicitly and thus obtain all the thermodynamic properties as a function of r and g. However, the complicated form of the integrand apparently makes this a formidable task, so we shall not attempt it here.

Instead, we shall use the same kind of scaling argument as reviewed in chapter 2 in the context of more conventional renormalization-group approaches. It should be strongly emphasized that it is not obvious that the transposition of these methods to the very unconventional form of action Eq.(3.30) is physically meaningful, and this remains a subject for future research. For now we take the view that it is, at least, interesting to examine the conclusions we can draw if the method is indeed justified.

3.3 Application to φ^4 Action: Potentially New Strongly Coupled Fixed Point

Since we have made the assumption to keep only the separable part of the action, the integration step is trivial as mentioned above. However, the remaining action must be rescaled and in general this step will not be a simple exercise in dimensional analysis since the basis functions are elliptic functions containing nontrivial dependence on the degrees of freedom.

We initiate the rescaling procedure by scaling the momentum magnitude $k' = bk$ where $b > 1$ and $k = 2\pi|\mathbf{n}|/L$. Assuming that we are calculating in the vicinity of a fixed point, the quantity $p_{\mathbf{n}}$ in Eq.(3.40) will scale as a power-law

$$p' = b^{d_p} p, \tag{3.42}$$

where d_p is the as-yet-unknown exponent and we have dropped the index $\mathbf{n}$ for brevity as the analysis from this point on concerns only the uniform scaling of the magnitudes and thus scalar quantities. Looking at the first term in Eq.(3.40) we find that after rescaling

$$\int d^d x p^2 c^2 \mathrm{sn}^2(px|m) \to \int d^d x' p'^2 \left(b^{d-2d_p} c^2\right) \mathrm{sn}^2(p'x'|m'), \tag{3.43}$$

where primed variables indicate post-rescaling, thus we find that

$$c'^2 = b^{d-2d_p} c^2 \tag{3.44}$$

defines the field amplitude scaling. Note that the term $p'x'$ in the elliptic function does *not* imply that $d_p = 1$. This is because the sn function is dependent on its modulus m, which also changes under rescaling. In fact, we can use Eq.(3.9) to relate p and m rescaling

$$
\begin{aligned}
p &= 4K(m)\frac{k}{2\pi} && (3.45)\\
b^{d_p}p \equiv p' &= \frac{2K(m')}{\pi}bk && (3.46)\\
\Rightarrow b^{d_p} &= \frac{K(m')}{K(m)}b, && (3.47)
\end{aligned}
$$

where we have combined the first two lines to obtain the third. Rearranging the last equality we obtain

$$
m' = K^{-1}(b^{d_p-1}K(m)). \tag{3.48}
$$

Recalling Eq.(3.8) we can further relate m and g resulting in

$$
\begin{aligned}
m' \equiv \frac{g'c'^2}{2p'^2} &= K^{-1}\left(b^{d_p-1}K\left(\frac{gc^2}{2p^2}\right)\right) && (3.49)\\
\Rightarrow \frac{c^2}{2p^2}g' &= b^{4d_p-d}K^{-1}\left(b^{d_p-1}K\left(\frac{c^2}{2p^2}g\right)\right), && (3.50)
\end{aligned}
$$

where we have used Eqs.(3.42,3.44) in the last line to simplify the resulting equation for g scaling. Absorbing the remaining terms in Eq.(3.40) into the rescaling of r, we find our final RG equation for r to be

$$
r' = b^{2d_p}r + b^{2d_p}\left(m - K^{-1}(b^{d_p-1}K(m))\right), \tag{3.51}
$$

where we have again used Eq.(3.8) to replace g with m.

3.4 Universal Characterization of Fixed Points in $d = 2, 3, 4$

We can use Eqs.(3.50,3.51) to identify fixed points (FP) of the theory. At such a point, the RG equations must simplify to $r' = r$ and $g' = g$. We find two solutions corresponding to $g \to 0$ and $g \to \infty$ or in terms of the elliptic modulus $m \to 0$ and $m \to 1$, which we denote as the Gaussian (G) FP and the strongly coupled (SC) FP respectively. This rescaling method utilized limiting values of r and g in order to generate the rescaling equations. The $d = 3$ critical point of φ^4 theory is expected to be located at finite values of r and g as given by, for example, ϵ-expansion methods in [42]. Therefore we will not discuss this FP further. Since $g' = g$ right at any FP, Eq.(3.50) simplifies as

$$\frac{c^2}{2p^2}g = b^{4d_p-d}K^{-1}\left(b^{d_p-1}K\left(\frac{c^2}{2p^2}g\right)\right) \tag{3.52}$$

$$\Rightarrow m = b^{4d_p-d}K^{-1}\left(b^{d_p-1}K(m)\right), \tag{3.53}$$

where we have again made use of Eq.(3.8). Now Eqs.(3.53,3.51) are both written in terms of m, which itself remains finite for both the Gaussian and the strongly coupled fixed point. This form of the rescaling equations is particularly helpful for identifying fixed points, but we want to make clear the relationship between the limiting values of m and g as we identify such points.

For the Gaussian fixed point we see that $g \to 0$ as $m \to 0$ from Eq.(3.9) using the fact that $K(m=0) = \pi/2$ in Eq.(3.8). Rewriting Eq.(3.53) at the Gaussian point $m' = m = 0$ we find

$$K\left(0b^{d-4d_p}\right) = b^{d_p-1}K(0) \tag{3.54}$$

$$\frac{\pi}{2} = \frac{\pi}{2}b^{d_p-1} \tag{3.55}$$

$$\Rightarrow b^{d_p-1} = 1 \tag{3.56}$$

$$\Rightarrow d_p = 1, \tag{3.57}$$

where the last line follows since $b > 1$ is arbitrary. In the limit of small m we can expand the elliptic integral $K(m)$ and the Eqs.(3.53,3.51) reduce to

$$\lim_{m\to 0} m'_G = b^{d_p-1}m \tag{3.58}$$

$$\lim_{m\to 0} r'_G = b^{2d_p}r, \tag{3.59}$$

where the subscript denotes that this is the Gaussian fixed point..

The strongly coupled fixed point can be found by first inverting a form of Eq.(3.53) when assuming that $m' = m$ as

$$\frac{1}{K(b^{d-4d_p}m)} = b^{1-d_p}\frac{1}{K(m)}. \tag{3.60}$$

This inversion is a necessary step, much as in section 9.6.6 of [15], since $K(m)$ diverges as $m \to 1$. However $K(m)$ is positive and finite when $m < 1$ therefore

$$1/K(1) = 0 \tag{3.61}$$

is the *only* value of $1/K(m)$ that vanishes. Plugging $m = 1$ into Eq.(3.60) and using Eq.(3.61) we obtain

$$\begin{aligned} \frac{1}{K(b^{d-4d_p})} &= 0 && (3.62)\\ \Rightarrow b^{d-4d_p} &= 1 && (3.63)\\ \Rightarrow d - 4d_p &= 0 && (3.64)\\ \Rightarrow d_p &= \frac{d}{4}, && (3.65) \end{aligned}$$

where we have again used the fact that $b > 1$ is arbitrary to go from line two to line three.

In the $m \to 1$ limit we also find that the m-dependence in Eq.(3.51) vanishes to give

$$\begin{aligned} \lim_{m\to 1} m'_{SC} &= b^{4d_p-d} m && (3.66)\\ \lim_{m\to 1} r'_{SC} &= b^{2d_p} r, && (3.67) \end{aligned}$$

which leads to $r^* = 0$ for both fixed points.

To identify the value of g for this strongly coupled fixed point we first use Eq.(3.9) to find that $\lim_{m\to 1} K(m) \to \infty$ implies that $\lim_{m\to 1} p \to \infty$. We then solve Eq.(3.8) for g and assume the amplitude c is finite to obtain $\lim_{m\to 1} g \to \infty$.

Therefore the fixed points (r^*, g^*) we identify here correspond to the Gaussian $(0, 0)$ and a new $(0, \infty)$ fixed point at strong $g \to \infty$ coupling. Using Eqs. (3.56,3.67) we immediately find the required values of d_p for each fixed point as

$$\begin{aligned} d_{p,G} &= 1 && (3.68)\\ d_{p,SC} &= \frac{d}{4}. && (3.69) \end{aligned}$$

Before calculating the power-law exponents for each of these points we characterize them based on the rescaling flows in their vicinity. We do this by choosing a point $r^* + \delta r$ and $m^* + \delta m$ near the corresponding fixed point while using the value for d_p obtained at that fixed point. We then apply Eqs.(3.48,3.51) to determine the direction of the resulting RG flows. Taking $m = 0 + \delta m$ at the Gaussian FP and $m = 1 - \delta m$

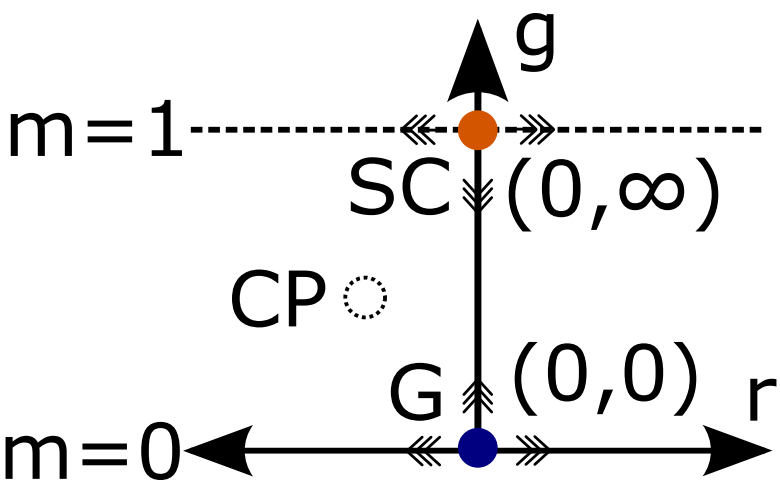

Figure 3.1: Flow diagram in the vicinity of Gaussian $(0,0)$ and strongly coupled $(0,\infty)$ fixed points in $d=3$. Axes are given as r vs g with corresponding values of m on the left. The dotted line represents the $m \to 1$ or $g \to \infty$ limit. Since flows in both cases are all away from each fixed point both points are unstable, but the SCFP exhibits a discontinuous ordering at the mean-field level whereas the Gaussian point does not indicate ordering even at mean-field.

at the SC FP, we find

$$m'_G = b^{4-d}\delta m \tag{3.70}$$

$$m'_{SC} = K^{-1}\left(b^{\frac{d-4}{4}}K(1-\delta m)\right). \tag{3.71}$$

As long as $d<4$ we find that for the Gaussian FP $m'>m$. Since $b^{\frac{d-4}{4}}<1$ and $K(m)$ is a strictly increasing function we find that for the strongly coupled FP $m'<m$. Although the equations near the Gaussian FP result in the expected mean field values, we see that the SC FP equations are marginal for $d \geq 4$. In order to address this new FP above the upper critical dimension we would likely need to include additional cross-terms in the action in Eq.(3.40). For either FP the equation for r is simple and flows away from $r^*=0$ in both directions. These fixed points and their corresponding flows in $d=3$ are given in Fig. 3.1.

In order to calculate the exponents for these fixed points, we first use the definition of the correlation exponent ν as the inverse of the largest eigenvalue of RG equations linearized near the fixed point. This is made especially simple given that Eqs.(3.58,3.59,3.66,3.67) for both fixed points decouple, thus we can read off ν from the scaling of r as

$$\nu = \frac{1}{2d_p}, \tag{3.72}$$

and the problem reduces to identifying d_p for each fixed point (see Eq. (3.68)) resulting in

$$\nu_G = \frac{1}{2} \tag{3.73}$$

$$\nu_{SC} = \frac{2}{d}. \tag{3.74}$$

Typically at least two exponents are needed to fully quantify the exponents at a given fixed point with the rest determined using scaling laws [20]. For the second exponent we use the definitions of η as the difference between the field scaling at the given fixed point and that at the Gaussian fixed point. This gives $\eta = 0$ by definition at the Gaussian point, but we can incorporate this result into a general formula as follows. In the eigensolution given in Eq.(3.6) the field scales as the amplitude c of the eigenfunctions. This scaling is fully determined by d_p as shown in Eq.(3.44). Setting the Gaussian value to $d_p = 1$ we find that

$$\frac{\eta}{2} = \frac{d - 2d_p}{2} - \frac{d-2}{2} \tag{3.75}$$

$$\Rightarrow \eta = 2(1 - d_p) = 0 \tag{3.76}$$

and for the strongly coupled fixed point, we obtain

$$\eta = 2 - \frac{d}{2}. \tag{3.77}$$

It is important to point out that traditionally the anomalous exponent η is defined as the deviation of the two-point Green function from mean field scaling. As such it describes the scaling of a linear response observable in the vicinity of a fixed point. The exponents β, γ, and δ are also attributed to linear response quantities. Typically a quantity such as η is calculated using the scaling of the Fourier field amplitudes, in accordance with the linear nature of the exponent. Since we are working with nonlinear basis functions here it is likely that our definition of η and thus β, γ, and δ via the scaling laws go beyond linear response theory and are not expected to be the same exponents as found using Fourier amplitude scaling. Table 3.1 summarizes all the exponents, however it is important to emphasize that η, β, γ, and δ are likely to change dramatically when the linear response part of the corresponding observable is extracted.

The SCFP in $d = 3$ is an unstable one like the Gaussian FP as is evident from the flow diagram in Fig. (3.1). Since the exponents are obtained from the exact eigenstates and such states form a complete basis [10], we have exactly characterized the strongly coupled fixed point. Further, unlike the Gaussian FP, the coupling $g \neq 0$ and thus there is the possibility of an ordered phase. In fact we can use a Landau-style argument to show that a discontinuous transition occurs at the mean-field level. To do this we write the

Table 3.1: φ^4 SC Exponents ($r = 0$, $g \to \infty$)

FP	G	SC
ν	$\frac{1}{2}$	$\frac{2}{d}$
η	0	$2 - \frac{d}{2}$
α	0	0
β	$\frac{1}{2}$	$\frac{1}{2}$
γ	1	1
δ	3	3

integrand of the action in Eq.(3.1) as

$$S = -\int d^d x \left\{ -\sigma \nabla^2 \sigma + r\sigma^2 + g\sigma^4 \right\}, \tag{3.78}$$

where σ now represents an order parameter for a Landau free energy described by S and we relax the periodic boundary constraint to allow for hyperbolic solutions as we will see below. Since the coupling g is arbitrarily large at the SCFP, we factor it out of the action to obtain

$$S = -g\int d^d x \left\{ -K\sigma \nabla^2 \sigma + R\sigma^2 + \sigma^4 \right\}, \tag{3.79}$$

where $K = 1/g$ and $R = r/g$ both have magnitudes much smaller than unity. When $R < 0$ the Eq.(3.79) has a stable solution representing the fact that the double well has created two new possible nonzero minima for $g > 0$ given by [31]

$$\varphi_0(x) = \pm\sqrt{\frac{R}{2}} \tanh\left(\sqrt{\frac{R}{K}} x\right). \tag{3.80}$$

When $r \geq 0$ then the minimum is about $\varphi = 0$, thus identifying the discontinuous shift between minima across $R = 0$.

It is important to note that, as discussed in section 5.5 of [15], this argument does **not** prove that the SCFP identified here is a discontinuous phase transition since the fluctuations neglected in such a mean field treatment have been known to be relevant and potentially alter the order of the transition. However, the presence of ordering at the mean-field level indicates that this FP is a transition and not simply a phase of the system. The analysis given above also indicates that the onset of soliton stability likely plays a significant role in the characterization of this fixed point at strong coupling.

Since the SCFP in $d = 3$ is unstable in every direction, a so-called doubly unstable fixed point as per [40], approaching it experimentally would be tricky as it requires fine-tuning both r and g or equivalently via Eqs.(rTherm-gTherm) the temperature T and details of the system in question such as the interaction

coupling J or the lattice spacing a for example. However, the signature of a fixed point is the onset of divergent observable quantites *in the vicinity* of said fixed point. In fact, of the exponents described in this work, only η is defined right at the fixed point since all other exponents describe divergence of their respective observables as the phase transition is approached. The instability of the SCFP presented here would then result in a type of crossover phenomena, see e.g. section 9.9 of [15] for typical examples, towards the critical point. Prior to the crossover, observables would then begin to scale as given by the SCFP exponents before ultimately scaling as those of the critical point.

A surprising consequence of the strongly coupled fixed point is that the exponents ν and α in $d = 2$ reduce exactly to those of Onsager's in the 2d Ising model. This may indicate that the fixed point in $d = 2$ is that of Onsager, but in order to prove this statement one would need to extract the linear response part of the elliptic basis functions at the SCFP. Once the linear part is calculated, then a comparison to the exponent $\eta = 1/4$ can be made, but such an extraction is beyond the scope of this work at this time. Of course for $d = 2$ it is possible that operators other than φ^4 are relevant and hence a careful analysis of this system includes higher order terms. However, the codimension of the Ising critical point is 2 [15] (two relevant directions) and these are in general the quadratic strength r and the external applied field H. If all of the remaining coupling parameters are found to be irrelevant then the universality class found here will remain unchanged. To check this we add terms such as $g_6\varphi^6, \cdots, g_{2i}\varphi^{2i}$ that obey the Ising symmetry to the action. The nonlinear eigenvalue procedure used to generate the complete basis for the $g_4\varphi^4$ theory above generalizes to the $g_{2i}\varphi^{2i}$ theory as well. We define this φ^{2i} hyperelliptic function by the inverse of the hyperelliptic integral

$$x = \int_0^{\varphi} \frac{dt}{\sqrt{(1-t^2)(1-m_1t^2)\cdots(1-m_{i-1}t^2)}} \tag{3.81}$$

where

$$\mathbf{m} = (m_1, m_2, \ldots, m_{i-1}) \tag{3.82}$$

and $\varphi = \mathrm{sn}_{2i}(x, \mathbf{m})$. The general solution to the nonlinear eigenvalue problem is given by

$$\varphi_n(\mathbf{x}) = c_n \ \mathrm{sn}_{2i}(\mathbf{p}_n \cdot \mathbf{x} + \theta_n, \mathbf{m}_n) \tag{3.83}$$

and the periodic boundary condition is satisfied by

$$\mathbf{p}_n = \frac{4K_{2i}(\mathbf{m}_n)n}{L} \tag{3.84}$$

where $K_{2i}(\mathbf{m}_n)$ is the hyperelliptic generalization to the complete elliptic integral of the first kind

$$\int_0^1 \frac{dt}{\sqrt{(1-t^2)(1-m_{1n}t^2)\cdots(1-m_{(i-1)n}t^2)}} \tag{3.85}$$

Inserting Eq.(3.83) with $i = 3$ into the nonlinear eigenvalue equation for φ^6 and equating like terms we find that

$$\begin{aligned}
\frac{g_4c^2}{2p^2} &= \tilde{m} && (3.86)\\
-\frac{g_6c^4}{3p^2} &= \bar{m} && (3.87)\\
\lambda &= p^2 + r + p^2(m_1 + m_2) && (3.88)\\
\Rightarrow \lambda &= p^2 + r + \frac{g_4c^2}{2} + \frac{g_6c^4}{3} && (3.89)
\end{aligned}$$

where $\tilde{m} = m_1 + m_2 + m_1m_2$ and $\bar{m} = m_1m_2$ and a similarly determined set of solutions obtain for the φ^{2i} case. Letting $m_1 \to 1$ and $m_2 \to 0$ while their product $m_1m_2 \to 0$ leads to the desired FP location where $\bar{m} \to 0$ and $\tilde{m} \to 1$. We then generate the rescaling equation analogous to Eq.(3.48)

$$K_6(\tilde{m}'b^{d-4d_p}, \bar{m}'b^{2d-6d_p}) = b^{d_p-1}K_6(\tilde{m}, \bar{m}) \tag{3.90}$$

and we see that $d_p = d/4$ and $d = 2$ gives

$$K_6(\tilde{m}', \bar{m}'b) = b^{-1/2}K_6(\tilde{m}, \bar{m}) \tag{3.91}$$

so that K_6 and $\bar{m}$ are both reduced upon rescaling showing that the φ^6 term is irrelevant. In general coefficients with $i > 2$ are irrelevant, supporting the claim that this is indeed the $d = 2$ Ising critical point.

One testable prediction of this strongly coupled fixed point is the value of the specific heat exponent. Because of the hyperscaling relation, $2 - \alpha = d\nu$, our computed value for $\nu = 2/d$ implies that $\alpha = 0$ as shown in Table (3.1). Consequently, the divergence is at best logarithmic. In addition, confirmation that the correlations diverge as $\nu = 2/d$ would further distinguish a transition from that of mean field, which also has $\alpha = 0$. The vanishing of the heat capacity is not a new phenomenon, but there are relatively recent developments in research regarding this situation and the corresponding logarithmic divergence accompanying it.

In the pnictides, a logarithmic divergence of the form $\ln|\mathrm{x}-\mathrm{x_c}|$ of the specific heat as a function of the doping parameter x in $BaFe_2(As_{1-x}P_x)_2$ has been seen in low fields [1, 26, 37]. A direct measurement of α would be preferable rather than in inference based on the effective mass since the very meaning of a quasiparticle is obscured in the local limit. In addition, care must be taken to distinguish a pure $\ln|\mathrm{T}|$ dependence from $T^a \ln|\mathrm{T}|$ as is observed in many non-Fermi liquid systems [9, 25, 33] in which $\alpha \neq 0$.

A scaling theory of the finite temperature Mott transition [3] has predicted that the heat capacity only has a $\ln|\mathrm{T}|$ dependence and as a result is well described by the $d = 2$ Ising exponents. What the strongly coupled fixed point identified here clarifies is that $\alpha = 0$ is a generic feature of a strongly coupled fixed point and not just the $d = 2$ Ising model. The applicability to Mott criticality is expected as such systems are governed by strong local interactions.

3.5 Analysis of Accessible Fixed Point Universality

The identification of this new fixed point is surprising and worthy of further general consideration. What other fixed points might be found using a complete nonlinear basis of states that separate the action? From the form of the RG equations Eqs.(3.51,3.48) and their generalizations to the $\varphi^2 n$ theory we can see that the separation of the action requires extreme values of the bare parameters r, g, and any higher order coefficients. As we have found a new fixed point for diverging g and vanishing r, we would suspect that there are fixed points at some if not all of the extreme values in physically allowed coefficient space.

3.6 Shortcomings of the Nonlinear Basis

We end by addressing the elephant in the room: which fixed points cannot be accessed by the method outlined above? As the astute reader might have noticed, we were careful to avoid discussion of the critical point and with good reason: it is not clear that this method cannot access it. As there are no additive terms in the interaction RG given by Eq.(3.48) this method will not be able to access any of the fixed points at

finite values of r, g, and higher coefficients. According to the results for the Wilson-Fisher fixed point given in the previous chapter, the $d = 3$ critical point in φ^4 theory is likely located in just such a region. Although one of the most important points in φ^4 theory is inaccessible to this method, the ability to explore strongly coupled fixed points in these models nonperturbatively is highly interesting in its own right. It is possible that higher order interactions have fixed points of a similar nature, and perhaps some of those are accessible to experiments as well.

Chapter 4

Renormalization Using the Limit of Finite Systems

Despite the successes of the nonlinear basis method, the lack of access to the $d = 3$ critical point in φ^4 theory motivates us to start over in an entirely new direction in our hunt for nonperturbative analytic solutions to the critical exponents. To that effect we return to discussion of the Wilsonian RG from early in Chapter 2. Recall that the key point of RG theory is to carefully handle the numerous divergences that crop up in a statistical mechanical system as one approaches the continuum limit on one hand and a critical phase transition on the other.

The first type of divergence has two diametrically opposed contributions to the singular nature of the model: the so-called UV and IR divergences. To deal with the UV divergence we define a sharp cutoff in momentum space. The Wilsonian RG method has a very clear physical interpretation for this: the sharp cutoff defines a working energy scale at which one discovers how the interactions in a theory at that scale modify the lower energy scales. This energy scale interpretation supports the choice of a hyperspherical shell in momentum space for the cutoff shape. One disadvantage of this cutoff choice is that integration of momentum space down to a lower momentum sharp cutoff will generate nonlocal terms in the action. Continuing with Wilson's original prescription, we will acknowledge this complication and address it once the RG equations are generated. However, the primary motivation for a sharp cutoff is practical in that it ensures each momentum state is either untouched or completely integrated over.

A sharp cutoff alone does not completely eliminate the singular nature of the action. We have addressed the UV divergence caused by arbitrarily high momentum values, but at the other end of the spectrum is the IR divergence caused by values of momentum approaching zero contributing a global constant value to the field in real-space. The most practical way to address this divergence is to enforce periodic boundary conditions on a finite system size L along each independent dimension in real-space

$$\varphi(x_i = L) = \varphi(x_i = 0) \; \forall \; i \in \{1, 2, \ldots, d\}. \tag{4.1}$$

We restate the φ^4 action as

$$\mathrm{S} = \int d^d x \Big\{ \Big(\nabla \psi(\mathbf{x}) \Big)^2 + r\psi(\mathbf{x})^2 + g\psi(\mathbf{x})^4 \Big\}, \tag{4.2}$$

where we have used ψ labels to be altered shortly. If we expand the field ψ in a Fourier transform

$$\psi(\mathbf{x}) = \frac{1}{L^d} \sum_{\mathbf{p}} \psi_{\mathbf{p}} e^{i\mathbf{p}\cdot\mathbf{x}}, \tag{4.3}$$

rescale via

$$\varphi(\mathbf{x}) = L^d \psi(\mathbf{x}), \tag{4.4}$$

and substitute these variables into Eq.(4.2) we obtain

$$\mathrm{S} \;=\; \int d^d x \Big(\sum_{\mathbf{p},\mathbf{p}'} (-\mathbf{p}\cdot\mathbf{p}' + r) \varphi_{\mathbf{p}} \varphi_{\mathbf{p}'} \; e^{i(\mathbf{p}+\mathbf{p}')\cdot\mathbf{x}} + g \sum_{\mathbf{m},\mathbf{n},\mathbf{p},\mathbf{q}} \varphi_{\mathbf{m}} \varphi_{\mathbf{n}} \varphi_{\mathbf{p}} \varphi_{\mathbf{q}} \; e^{i(\mathbf{m}+\mathbf{n}+\mathbf{p}+\mathbf{q})\cdot\mathbf{x}} \Big). \tag{4.5}$$

We then integrate over real space using

$$\int d^d x \; e^{i\mathbf{k}\cdot\mathbf{x}} = L^d \delta(\mathbf{k}) \tag{4.6}$$

to obtain

$$\mathrm{S} = L^d \Big(\sum_{\mathbf{m}} 2(p_{\mathbf{m}}^2 + r) \varphi_{-\mathbf{m}} \varphi_{\mathbf{m}} + g \sum_{\mathbf{m},\mathbf{n},\mathbf{p},\mathbf{q}} \varphi_{\mathbf{m}} \varphi_{\mathbf{n}} \varphi_{\mathbf{p}} \varphi_{\mathbf{q}} \; \delta(\mathbf{m}+\mathbf{n}+\mathbf{p}+\mathbf{q}) \Big), \tag{4.7}$$

where

$$p_{\mathbf{m}}^2 = (2\pi|\mathbf{m}|)^2 / L^2 \tag{4.8}$$

are the only allowed values of momentum due to the periodic boundary with $\mathbf{m} = (m_1, m_2, \ldots, m_d)$ a set of vector-valued integers representing a point in momentum space. Note that the quadratic part is reduced to a simple sum whereas the quartic part is still fairly complicated. The field variable $\varphi_{\mathbf{n}}$ is the Fourier amplitude of the real-valued field $\varphi(\mathbf{x})$ for momentum $p_{\mathbf{n}}$ and the delta function enforces translational invariance. Second, taking the limit $\lim L \to \infty$ while holding the sharp cutoff magnitude Λ constant, where $|p_{\mathbf{m}}| \in [0, \Lambda]$, recovers the continuum field theory model. This can be seen by noting that the number of $\varphi_{\mathbf{m}}$ variables with $|p_{\mathbf{m}}| \leq \Lambda$ increases with L. Finally, we choose a scale parameter $b > 1$ representing a sharp

splitting between the 'fast' modes to be integrated over $\varphi_{\mathbf{M}}$ with $|p_{\mathbf{M}}| \in [\Lambda/b, \Lambda]$ and the 'slow' modes left after the coarse-graining step $\varphi_{\mathbf{m}}$ with $|p_{\mathbf{m}}| \in [0, \Lambda/b]$. This results in a finite number of degrees of freedom in the integration step for finite values of L. Notice our notation where the fast modes are represented by capital indices and slow modes by lowercase indices. We will continue this notation throughout the chapter. The last two advantages given above may seem less like advantages and more like unnecessary redundant steps. After all, our goal is the analytic calculation of observables in the continuum theory, so should we take the continuum limit all over again and lose any advantage gained by the finite system description? We claim that the continuum model taken as a whole contains far more information than is experimentally accessible and so should not be viewed as containing observable information that the limit of the finite system does not already contain. We first use a finite-system model to calculate the physical observables of interest and only then take the continuum limit. Along the way we check that each step self-consistently converges to the continuum limit system and that the RG equations and physical observables obtained in this way are analytic and devoid of singular values. Provided that all of these requirements are met, we claim that the result is that of the continuum system without ever having actually worked with the continuum theory itself! Lastly, it is important to mention that the finite system strictly speaking cannot obey the requirements set by RG. For example the momentum lattice values, when rescaled, cannot perfectly recover the original range of momentum values. In particular the lowest magnitude momenta $|p| = d(2\pi/L)$ are rescaled to larger values than they were initially with no replacements below them to take their place. This approximate RG is typical of such a finite system and systematically converges to the requirements of RG in the continuum limit.

This approach is akin to a type of lattice regularization albeit in momentum space and not that of the far more common real-space lattice regularization approach. Even so, the so-called fast modes in the partition function in Eq.(2.23) represented by the Fourier series lattice in Eq.(4.7) still form a formidable barrier to integration. This is the point at which some type of perturbative series is typically invoked in order to proceed. The use of the perturbative approach is ubiquitous and powerful due primarily to two key properties. First, it expands about a well-known and exactly-solved action, typically a type of free-field theory. This ensures that the starting point of the expansion is well understood conceptually. Second, it generates a series of solvable Gaussian integrals, providing a practical and algorithmic procedure to compute observables of interest. Gaussian integration here is extremely powerful, especially given that the general form of the partition function nearly guarantees the inevitable need to integrate over exponentials of a Gaussian or more complex nature.

What we want to do is keep this powerful tool of Gaussian integration at our disposal while relaxing the

requirement of expanding about a free-field theory. In other words, we want to formulate an expansion about a parameter that does not significantly alter the form of the interactions in the original action. Therefore we must not expand about the coupling coefficient $g = 0$ in Eq.(2.22). We are certainly not the first to try using alternative parameters to retain the powerful Gaussian integration toolset. The $\epsilon = 4 - d$ expansion near the upper critical dimension and the $1/N$ expansion in large O(N) symmetry are well-known examples of perturbative parameters other than the coupling strength. However, we wish to develop a method applicable to a wide range of interacting models allowing for general variations in symmetry groups, field-type, and dimension.

Having already discussed that the system size itself will be taken to the infinite limit at the end of the calculation we find that the system volume L^d is exactly the parameter we are looking for, which has been made clear by the form of the action in Eq.(4.7). Note that the gradient term has a factor of L^{-2}, but the restriction of the momentum to $p \in (0, \Lambda)$ limits the values p can take to a finite range. Proceeding with the RG we need to formally average over the fast modes by writing the partition function as

$$Z = Z_> \int D[\varphi_<] \Big\{ e^{-\mathrm{S}_<} \Big(\frac{\int D[\varphi_>] e^{-\mathrm{S}_{\mathrm{mix}}}}{\int D[\varphi_>] e^{-\mathrm{S}_>}} \Big) \Big\}, \tag{4.9}$$

using the following definitions

$$\begin{aligned}
Z_> &= \int D[\varphi_>] e^{-\mathrm{S}_>} && (4.10)\\
\mathrm{S}_{\mathrm{shell}} &\equiv \mathrm{S}\Big(|p_{\mathbf{k}}| \in [0, \Lambda] \Big) && (4.11)\\
\mathrm{S}_> &\equiv \mathrm{S}\Big(|p_{\mathbf{k}}| \in [\frac{\Lambda}{b}, \Lambda] \Big) && (4.12)\\
\mathrm{S}_< &\equiv \mathrm{S}\Big(|p_{\mathbf{k}}| \in [0, \frac{\Lambda}{b}] \Big) && (4.13)\\
\mathrm{S}_{\mathrm{mix}} &\equiv \mathrm{S}_{\mathrm{shell}} - \mathrm{S}_<, && (4.14)
\end{aligned}$$

where S is defined as in Eq.(4.7), $|p_{\mathbf{k}}|$ is the magnitude of the momentum at the corresponding indexed location $\mathbf{k}$, $p_{\mathbf{k}}$ is given by Eq.(4.8), and we have also used

$$\begin{aligned}
D[\varphi_<] &= \prod_{|p_{\mathbf{k}}| \in [\frac{\Lambda}{b}, \Lambda]} d\varphi_{\mathbf{k}} && (4.15)\\
D[\varphi_>] &= \prod_{|p_{\mathbf{k}}| \in [0, \frac{\Lambda}{b}]} d\varphi_{\mathbf{k}}. && (4.16)
\end{aligned}$$

4.1 Lattice Regularization in the Continuum Limit: Laplace's Method

We can now use the fact that the system volume can be taken to arbitrarily large values to formally expand S in a series about $L^{-d} = 0$

$$\int D[\varphi_>] e^{-L^d \mathrm{S}} = \; L^{-d/2} \sqrt{\frac{-2\pi}{\det \mathcal{H}[\varphi_0]}} e^{-L^d \mathrm{S}[\varphi_0]} + \mathcal{O}(L^{-d}), \tag{4.17}$$

where $\mathcal{H}$ is the Hessian with respect to the fast fields

$$\mathcal{H} = \sum_{IJ} \frac{\partial \mathrm{S}}{\partial \varphi_I \partial \varphi_J}, \tag{4.18}$$

and φ_0 represents the value of the global minima for all fast modes. Although Eq.(4.17) is similar in mathematical form to other perturbative methods, conceptually it is entirely different. Eq.(4.17) is formally divergent just like an expansion about $g = 0$ for example, but the difference is in the interpretation of what each term contributes to the calculation of physical observables.

When expanding about $g = 0$ the lowest order term is the free-field theory, an exactly solved and well understood theory. On the other hand the higher order terms contain corrections to the free theory when interactions are turned on. Most importantly these corrections contain the much sought-after information regarding the changes to the physical observables for the interacting theory. Unfortunately these terms are formally divergent and fated to eventually provide inadequate accuracy in describing the physical variables when the interactions are not arbitrarily weak. This is a ubiquitous issue throughout field theory research, and much effort has been made to push the point at which this divergence begins to cause discrepancy to higher and higher order. Recent use of conformal bootstrap methods has increased the precision of the critical exponents from about 3 decimal places to several more, but there again it seems to hit a limitation. The lowest term in an expansion about $L^{-d} = 0$, however, corresponds exactly to the full contribution in the infinite system limit. We have given up the conceptually clear free theory from which to expand around and gained mathematical tractability while avoiding the need to address the inevitable divergence of the expansion terms. In our case these formally divergent higher order terms merely encode corrections for the case of a finite system. Provided that we can compute the exact exponent contribution from the first term in our expansion, we will have found the exact final result for the exponents in the vicinity of the φ^4 continuum theory critical point. The benefits of such a result are hard to overstate. Of particular interest is the identification of precisely what microscopic degrees of freedom directly contribute to the deviation of

the critical exponents from those of mean field theory for example.

The first term in Eq.(4.17) is the solution to the multidimensional form of Laplaces method where we have used the system volume L^d as the required arbitrarily large parameter. Since we are ultimately interested in how this integration step modifies the remaining modes of the original action we can rewrite the result of Laplaces method so that all remaining field variables are found in the exponent as

$$\mathrm{S}'_{\mathrm{int}} = -L^d\Big\{\mathrm{S}[\varphi_0] + \frac{1}{2L^d}\ln\left(\det\mathcal{H}[\varphi_0]\right)\Big\}. \tag{4.19}$$

Using Eq.(4.19) in the average given in Eq.(4.9) we obtain the final formal result

$$\mathrm{S}_{\mathrm{int}} = -L^d\Big\{\mathrm{S}_{\mathrm{mix}}[\varphi_{0,\mathrm{mix}}] - \mathrm{S}_{>}[\varphi_{0,>}] + \frac{1}{2L^d}\ln\left(\frac{\det\mathcal{H}[\varphi_{0,\mathrm{mix}}]}{\det\mathcal{H}[\varphi_{0,>}]}\right)\Big\}. \tag{4.20}$$

Our goal is made clear in Eq.(4.20). We must identify the global minimum solution of the fast modes in the infinite volume limit for S_{mix} and $S_{>}$. Then we compute the Hessian of each action with respect to the fast modes and evaluate it at its respective global minimum. Finally, we will need to expand the logarithm of the determinant of the Hessian for S_{mix} given in Eq.(4.20) in powers of the slow modes $\varphi_{<}$ to identify contributions to the RG equations modifying the coefficients r and g in $S_{<}$.

The procedure outlined above is reminiscent of Green function expansion methods often encountered in perturbative field theory, but it is not directly comparable. We are not expanding about a free-field theory, and correspondingly there is no clear free propagator with which we can separate contributions to the renormalization of the action. Using a nonperturbative analytic method to calculate results in a strongly coupled system seems likely to have little if anything to do with the corresponding free field theory in any case.

4.2 Formulating RG Equations

Now that we have a formal solution to the coarse-graining step given by Eq.(4.20), we can proceed with a rescaling of the momenta and find RG equations for a general action S! Since we are using a sharp momentum cutoff Λ as well as a sharp boundary between integrated and unintegrated momenta Λ/b, the rescaling step is fairly straightforward. We rescale the momenta by a factor $|\mathbf{k}'| = b|\mathbf{k}|$ and further define

$$\varphi'_{\mathbf{k}'} = z\varphi_{\mathbf{k}}, \tag{4.21}$$

where z is the as-of-yet unknown field renormalization. Suppose that the expansion of the coarse-graining result given by Eq.(4.20) results in

$$\mathrm{S_{int}} = -L^d \left\{ \sum_{\mathbf{k}} \left(Ak^2 \varphi_{\mathbf{k}}^2 + B\varphi_{\mathbf{k}}^2 \right) + \sum_{\mathbf{k,l,m,n}} C\delta(\mathbf{k}+\mathbf{l}+\mathbf{m}+\mathbf{n})\varphi_{\mathbf{k}}\varphi_{\mathbf{l}}\varphi_{\mathbf{m}}\varphi_{\mathbf{n}} + \mathcal{O}(k^4\varphi^2, k^2\varphi^4, \varphi^6) \right\}, \quad (4.22)$$

where we have further expanded the result in powers of slow momenta k^2 in order to extract the term that renormalizes the gradient. In this case A, B, and C are in general functions of Λ, b, and L as well as r and g. Then combining Eqs.(4.21,4.22) we first absorb all changes to the gradient term into z giving

$$z = b^{(d-2)/2} \left(1 + A\right), \quad (4.23)$$

where the power of b comes from the rescaling of L^d and the factor k^2. Similarly we can absorb changes in the quadratic and quartic terms into redefinitions of r and g as

$$r' = b^d z^{-2} \left(r + B\right) \quad (4.24)$$

$$g' = b^d z^{-4} \left(g + C\right). \quad (4.25)$$

Eqs.(4.23-4.25) comprise our RG equations, and it remains to calculate A, B, and C for a given action S via an expansion of Eq.(Eq10). The above analysis and it's results are quite general and are not dependent on our choice of integration method described in the previous section. Eqs.(4.23-4.25) are simply the general forms for rescaling φ^4 theory when using a sharp cutoff. Taken as a whole, the RG procedure described here is new in that $\mathrm{S_{int}}$ in Eq.(4.20) is a formally exact expression for the integration step. If one can calculate $\mathrm{S_{int}}$ exactly, that is without approximation or truncation, to the order required in Eq.(4.22) then the resulting values of A, B, and C will likewise be determined exactly for that action.

4.3 RG for a Reduced φ^4 Model

Calculating the results of Eq.(4.20) for the action given by Eq.(4.7) is underway but not complete as of this work. In order to showcase the application of the method outlined above, and to examine its benefits, we will use a reduced form of Eq.(4.7) given by

$$\tilde{S} = L^d\Big(\sum_{\mathbf{m}} 2(p_{\mathbf{m}}^2 + r)\varphi_{-\mathbf{m}}\varphi_{\mathbf{m}} + 6g\sum_{\mathbf{m},\mathbf{n}} \varphi_{\mathbf{m}}\varphi_{-\mathbf{m}}\varphi_{\mathbf{n}}\varphi_{-\mathbf{n}}\Big). \tag{4.26}$$

The action $\tilde{S}$ contains only quartic terms that can be written as powers of the quadratic term. This is no longer the Fourier transform of the semi-local real-space field $\varphi(\mathbf{x})$. Extending $\tilde{S}$ by higher powers of the quadratic term $\sum_{\mathbf{m}} \varphi_{\mathbf{m}}\varphi_{-\mathbf{m}}$, however, creates an action that is closed under RG in the Wilsonian sense. By this we mean that coarse-graining will not introduce quartic or higher order terms other than those proportional to an expansion in powers of $\sum_{\mathbf{m}} \varphi_{\mathbf{m}}\varphi_{-\mathbf{m}}$.

In order to proceed, it is helpful to first transform to real and imaginary parts of the field variables $\varphi_{\mathbf{m}}$ and $\varphi_{-\mathbf{m}}$ as

$$\varphi_{\mathbf{m}} = Re[\varphi_{\mathbf{m}}] + iIm[\varphi_{\mathbf{m}}] \tag{4.27}$$

$$\varphi_{-\mathbf{m}} = Re[\varphi_{\mathbf{m}}] - iIm[\varphi_{\mathbf{m}}], \tag{4.28}$$

or for brevity

$$\varphi_{\mathbf{m}} \equiv R_{\mathbf{m}} + iI_{\mathbf{m}} + \tag{4.29}$$

$$\varphi_{-\mathbf{m}} \equiv R_{\mathbf{m}} - iI_{\mathbf{m}}. \tag{4.30}$$

The term $\varphi_{\mathbf{m}}\varphi_{-\mathbf{m}}$ originated from real function $\varphi(\mathbf{x})$ and thus, as can be seen in Eqs.(4.29,4.30), $\varphi_{\mathbf{m}}$ and $\varphi_{-\mathbf{m}}$ are not independent variables. $R_{\mathbf{m}}$ and $I_{\mathbf{m}}$, however, are independent provided the sum over momenta is restricted to a half-hypersphere. The numerical factors that this change of variables imparts to the measure $D[\varphi]$ are irrelevant for the RG and cancel due to the averaging in Eq.(4.9) in either case.

Using the substitution

$$\varphi_{\mathbf{m}}\varphi_{-\mathbf{m}} = R_{\mathbf{m}}^2 + I_{\mathbf{m}}^2 \tag{4.31}$$

$$\equiv z_{\mathbf{m}}^2 \tag{4.32}$$

we can begin the coarse-graining procedure by calculating the multivariable extrema of $\tilde{S}_{\text{mix}}$ as

$$0 = \frac{\partial \tilde{S}_{\rm mix}}{\partial R_{\mathbf{M}}} = 4R_{\mathbf{M}}\left(\Lambda^2 + r + 12gf\right) + 24gR_{\mathbf{M}}\sum_{\mathbf{N}\neq\mathbf{M}} z_{\mathbf{N}}^2 + 24gz_{\mathbf{M}}^2 R_{\mathbf{M}} \tag{4.33}$$

$$0 = \frac{\partial \tilde{S}_{\rm mix}}{\partial I_{\mathbf{M}}} = 4I_{\mathbf{M}}\left(\Lambda^2 + r + 12gf\right) + 24gI_{\mathbf{M}}\sum_{\mathbf{N}\neq\mathbf{M}} z_{\mathbf{N}}^2 + 24gz_{\mathbf{M}}^2 I_{\mathbf{M}}, \tag{4.34}$$

where we have resumed the use of capital letters to represent fast modes and assumed that the fast mode shell is thin $b-1 \ll 1$ and thus all fast modes are at magnitude Λ. We have also defined the sum over quadratic slow modes as

$$f \equiv \sum_{\mathbf{m}} R_{\mathbf{m}}^2 + I_{\mathbf{m}}^2 \tag{4.35}$$

$$f = \sum_{\mathbf{m}} z_{\mathbf{m}}^2 \tag{4.36}$$

and thus

$$f^2 = \sum_{\mathbf{m},\mathbf{n}} z_{\mathbf{m}}^2 z_{\mathbf{n}}^2 \tag{4.37}$$

for brevity. The solutions to Eqs.(4.33,4.34) are given by

$$R_{\mathbf{M}}^2 = I_{\mathbf{M}}^2 = 0 \text{ or} \tag{4.38}$$

$$R_{\mathbf{M}}^2 + I_{\mathbf{M}}^2 = -\frac{c_0 + 2f}{N} \tag{4.39}$$

for each $\mathbf{M}$, where $c_0 = (\Lambda^2 + r)/6g$ and N is now the number of fast modes that are nonzero. Thus if there are T total fast modes then there are 2^T total extrema given by N modes with $z_{\mathbf{M}} \neq 0$ and $T - N$ modes with $z_{\mathbf{M}} = 0$, where $N \in 1, 2, \ldots, T$.

Substituting Eq.(4.39) into $\tilde{S}_{\rm mix}$ we find that

$$\tilde{S}_{\rm mix}(N) = -6g(c_0 + 2f)^2, \tag{4.40}$$

which is independent of N. The global minimum corresponds to the most negative value of $\tilde{S}_{\rm mix}(N)$ *provided* the Hessian is positive at that solution. As an example, calculating the Hessian for $\tilde{S}_{\rm mix}(N = 1)$ we find

$$\frac{\mathcal{H}(\tilde{S}_{\rm mix}(N=1))}{12g} = \begin{bmatrix} c_0+2f+z_1^2+2R_1^2 & 2R_1I_1 & 0 & 0 & 0 & \dots & 0 \\ 2R_1I_1 & c_0+2f+z_1^2+2I_1^2 & 0 & 0 & 0 & \dots & 0 \\ 0 & 0 & c_0+2f & 0 & 0 & \dots & 0 \\ 0 & 0 & 0 & c_0+2f & 0 & \dots & 0 \\ \vdots & \vdots & \vdots & \vdots & \ddots & \vdots & \vdots \\ 0 & 0 & 0 & 0 & \dots & c_0+2f & 0 \\ 0 & 0 & 0 & 0 & \dots & 0 & c_0+2f \end{bmatrix}, \tag{4.41}$$

where WLOG we have assumed that the nonzero $z_{\mathbf{M}}$ was the first one. Here we run into a problem because the determinant is zero! In particular one of the eigenvalues of this matrix is zero. This is true even for $N > 1$.

Not all hope is lost, however, as there is evidence that a change of variables is in order. We can see this by noting that the action at the minimum is a function of $z_{\mathbf{M}}^2 = R_{\mathbf{M}}^2 + I_{\mathbf{M}}^2$ only. If we make the transformation to polar coordinates

$$z_{\mathbf{M}}^2 = R_{\mathbf{m}}^2 + I_{\mathbf{m}}^2 \tag{4.42}$$

$$\tan(\theta_{\mathbf{M}}) = \frac{I_{\mathbf{m}}}{R_{\mathbf{m}}} \tag{4.43}$$

only for the nonzero fast mode, then our extrema equation becomes

$$0 = \frac{\partial \tilde{S}'_{\rm mix}}{\partial R_{\mathbf{M}}} = 4z_{\mathbf{M}}\left(\Lambda^2 + r + 12gf\right) + 24gz_{\mathbf{M}}\sum_{\mathbf{N}\neq\mathbf{M}} z_{\mathbf{N}} + 24gz_{\mathbf{M}}^3. \tag{4.44}$$

If we further assume all but one $z_M = 0$ for example then the remaining nonzero solution becomes

$$z_M^2 = -(c_0 + 2f). \tag{4.45}$$

This results in the same minimum as in Eq.(4.40). If we now integrate out $\theta_{\mathbf{M}}$ and *then* calculate the new Hessian we find that it is diagonal resulting in a total contribution from the integration of the fast modes given by

$$\sum_{\mathbf{K}} z_{\mathbf{K}} \det \mathcal{H}_{\rm polar}(\tilde{S}_{\rm mix}(N=1)) e^{-L^d \tilde{S}_{\rm mix}(N=1)} = -T \frac{(c_0+2f)}{\sqrt{12g}} \Big(12g(c_0+2f)\Big)^{1-T} e^{L^d(6g(c_0+2f)^2)}, \qquad (4.46)$$

where the sum combines all possible $N=1$ solution points, $\tilde{S}_{\rm mix}(N=1)$ is now a function of $z_{\mathbf{K}}$, and $\mathcal{H}_{\rm polar}$ is the Hessian of our transformed action $\tilde{S}'_{\rm mix}(N=1)$. We can factor out all dependence on the slow modes given by f outside the exponential in Eq.(4.46) as

$$-T\sqrt{\frac{(c_0+2f)}{12g}}\Big(12g(c_0+2f)\Big)^{1-T} = -T(12g)^{1/2-T} c_0^{3/2-T} (1+\frac{2f}{c_0})^{3/2-T}. \qquad (4.47)$$

Exponentiating the logarithm of the f-dependent term in Eq.(4.47) and factoring out $-L^d$ provides a contribution

$$-\frac{1}{L^d}\ln\Big((1+\frac{2f}{c_0})^{3/2-T}\Big) \approx \frac{T-3/2}{L^d}\Big(\frac{2f}{c_0} - 2\left(\frac{f}{c_0}\right)^2 + \mathcal{O}(f^3)\Big), \qquad (4.48)$$

where we have neglected a term independent of f when going from Eq.(4.46) to Eq.(4.48).
T represents the number of fast mode momentum points approximating the surface of a hyperspherical shell at radius Λ, and for our thin-shell cutoff procedure the volume of this shell is the thickness δb times the surface of the d-dimensional hypersphere denoted S_{d-1} with radius Λ. In the continuum limit $T \to \infty$ as $L \to \infty$ and each point in momentum space has volume $(2\pi/L)^d$. Therefore the quantity $\frac{T-3/2}{L^d}$ appearing in Eq.(4.48) in the continuum limit becomes

$$V \equiv \frac{S_{d-1}\Lambda^{d-1}}{(2\pi)^d}. \qquad (4.49)$$

Combining Eq.(4.48) with the action already in the exponential in Eq.(4.46) we find that to $\mathcal{O}(f^2)$ our contribution from the integration step becomes

$$-L^d\Big\{V\delta b\frac{2f}{c_0} - 2V\delta b\left(\frac{f}{c_0}\right)^2 - 12gc_0 f - 144gc_0^2 f^2\Big\}. \qquad (4.50)$$

Using the definitions for powers of f given by Eqs.(4.36,4.37) as well as $c_0 = (\Lambda^2 + r)/6g$ and recalling Eq.(4.26) to determine the original coefficients of the theory and factor them out of the terms in this expansion we obtain

$$-12gc_0f + V\delta b\frac{2f}{c_0} = 2f\Big(-2(\Lambda^2+r) + 6V\delta b\Big(\frac{g}{\Lambda^2+r}\Big)\Big) \tag{4.51}$$

$$-24gf^2 - 2V\delta b\left(\frac{f}{c_0}\right)^2 = 6f^2\Big(-4g - 12V\delta b\Big(\frac{g}{\Lambda^2+r}\Big)^2\Big) \tag{4.52}$$

We thus find the quantities A, B, and C from Eqs.(4.23-4.25) as

$$A = 0 \tag{4.53}$$

$$B = -2(\Lambda^2+r) + 6V\delta b\Big(\frac{g}{\Lambda^2+r}\Big) \tag{4.54}$$

$$C = -4g - 12V\delta b\Big(\frac{g}{\Lambda^2+r}\Big)^2, \tag{4.55}$$

where the first term comes from the minimum of the action, the second term comes from the expansion of the logarithm of the Hessian, and we have used the quantity V from Eq.(4.49).

Although it seems that we have what we've been seeking, this is not the case as there is a fatal flaw in Eqs.(4.23-4.25) when applying Eqs.(4.53-4.55). Due to the contributions from the negative action at the global minimum, there is a constant additive term in the equation for r as well as a sign flip in the first term of the equation for g. These changes ensure that there is no fixed point solution at $(r, g) = (0, 0)$ and the only finite fixed point solution requires $g < 0$, which is a nonphysical part of coupling space! How can we rectify such serious problems? Since the culprit comes from the value of the action at the global minimum being less than zero for $g > 0$, it is time to switch from a purely mathematical analysis of the extrema generated by Laplace's method here and analyze the system with respect to physical constraints.

It is true that in the limit $L \to \infty$ the global minimum of the action *can* be negative, but what we have shown is that there no fixed points in this case under the constraint that $g > 0$. In other words, there are no self-similar points and thus no singular behavior at such extrema. Since we are only interested in singular behavior of the partition function arising from a self-similar solution to the RG equations, we must revise our method and subsequent use of Laplace's method: expand about the extrema that minimize the action *subject to the constraint* that such extrema identify self-similar singular behavior. In general we find that for the action given in Eq.(4.26) *any* extrema that correspond to negative values of the action when $g > 0$ do not generate fixed points. Thus the global extremum containing fixed point solutions in physical parameter space corresponds to the *other* set of solutions to the extrema equations given by Eq.(4.38), which is also conveniently a much easier point to solve.

Since $\tilde{S}_{\rm mix}$ contains only terms with at least one fast mode plugging in Eq.(4.38) results in

$$\tilde{S}_{\rm mix}(z_{\mathbf{M}}=0)=0, \tag{4.56}$$

where we have assumed all fast modes are set to zero. To determine the Hessian we can start with Eqs.(4.33,4.34) and take one more derivative with respect to real and imaginary parts for each giving

$$\begin{aligned}
\frac{\partial^2\tilde{S}_{\rm mix}}{\partial R_{\mathbf{M}}\partial I_{\mathbf{N}}}(z_{\mathbf{M}}=0) &= 4(\Lambda^2+r+12gf)\equiv 12g(c_0+2f) &(4.57)\\
\frac{\partial^2\tilde{S}_{\rm mix}}{\partial R_{\mathbf{M}}\partial I_{\mathbf{N}}}(z_{\mathbf{M}}=0) &= 4(\Lambda^2+r+12gf)\equiv 12g(c_0+2f) &(4.58)\\
\frac{\partial^2\tilde{S}_{\rm mix}}{\partial R_{\mathbf{M}}\partial I_{\mathbf{N}}}(z_{\mathbf{M}}=0) &= 0, &(4.59)
\end{aligned}$$

where we have again used

$$c_0\equiv\frac{\Lambda^2+r}{6g}. \tag{4.60}$$

We thus find that the Hessian becomes

$$\frac{\mathcal{H}_0(\tilde{S}_{\rm mix})}{12g}=\begin{bmatrix}
c_0+2f & 0 & 0 & 0 & 0 & \dots & 0\\
0 & c_0+2f & 0 & 0 & 0 & \dots & 0\\
0 & 0 & c_0+2f & 0 & 0 & \dots & 0\\
0 & 0 & 0 & c_0+2f & 0 & \dots & 0\\
\vdots & \vdots & \vdots & \vdots & \ddots & \vdots & \vdots\\
0 & 0 & 0 & 0 & \dots & c_0+2f & 0\\
0 & 0 & 0 & 0 & \dots & 0 & c_0+2f
\end{bmatrix},$$

where the subscript on $\mathcal{H}_0$ indicates that we are applying the solution in Eq.(4.38) to the Hessian calculated using the original fast mode variables $R_{\mathbf{M}}$ and $I_{\mathbf{M}}$. Therefore the determinant of the Hessian of $\tilde{S}_{\rm mix}(z_{\mathbf{M}}=0)$ in this case becomes

$$\Big(12g(c_0+2f)\Big)^{2T}, \tag{4.61}$$

where T is the number of fast modes $\mathbf{M}$ and the factor of 2 in the exponent comes from the fact that each fast mode has real and imaginary components.

Since Eq.(4.56) shows that only the Hessian contributed to the integration step we simply take the exponential of the logarithm of

$$\frac{2\pi}{\sqrt{\Big(12g(c_0+2f)\Big)^{2T}}} = 2\pi\Big(12g(c_0+2f)\Big)^{-T}, \tag{4.62}$$

which becomes

$$\exp\Big\{\ln(2\pi(12gc_0)^{-T}) - T\ln(1+\frac{2f}{c_0})\Big\}. \tag{4.63}$$

When we calculate the same integration step for $\tilde{S}_>(z_{\mathbf{M}}=0)$ the only difference is that $f=0$. Dividing the integration of $\tilde{S}_{\rm mix}$ by that of $\tilde{S}_>$ simply cancels the first term in Eq.(4.63). When we factor out $-L^{-d}$ and then take the limit as $T\to\infty$ the expansion of the logarithm in powers of f is the same as in Eq.(4.48). We can then factor out $2f$ and $6f^2$ from the first two terms in the expansion respectively in the same way as given by Eqs.(4.51,4.52) to obtain

$$\begin{aligned} A &= 0 && (4.64)\\ B &= 6V\delta b\Big(\frac{g}{\Lambda^2+r}\Big) && (4.65)\\ C &= -12V\delta b\Big(\frac{g}{\Lambda^2+r}\Big)^2. && (4.66) \end{aligned}$$

This result differs from Eqs.(4.53-4.55) in that it is devoid of the troublesome terms not proportional to $V\delta b$. We can now turn to finding the fixed point solutions of the RG equations, but to make things even more clear we can transform these recursion relations to differential equations by simply performing a Taylor expansion with respect to b about $b=1$ in the thin shell limit as

$$\begin{aligned} r' &= r+\Big(2r+6V\frac{g}{\Lambda^2+r}\Big)\delta b+\mathcal{O}(\delta b^2) && (4.67)\\ g' &= g+\Big((4-d)g-12V\Big(\frac{g}{\Lambda^2+r}\Big)^2\Big)\delta b+\mathcal{O}(\delta b^2) && (4.68)\\ \Rightarrow \frac{dr}{db} &= 2r+6V\frac{g}{\Lambda^2+r} && (4.69)\\ \frac{dg}{db} &= (4-d)g-12V\Big(\frac{g}{\Lambda^2+r}\Big)^2, && (4.70) \end{aligned}$$

where $\delta b \ll 1$. Besides simplifying the equations themselves, the advantage to this form for the RG equations

is the fixed point solutions simply require

$$\frac{dr}{db} = 0 \tag{4.71}$$
$$\frac{dg}{db} = 0, \tag{4.72}$$

which are given by

$$(r^*, g^*) = (0, 0) \tag{4.73}$$
$$(r^*, g^*) = \Big(-\frac{4-d}{8-d}\Lambda^2, \frac{4-d}{(8-d)^2}\frac{4\Lambda^4}{3V} \Big). \tag{4.74}$$

Notice that we obtain the Gaussian point at the origin as well as a nontrivial solution dependent on Λ and V. The dependence of r^* and g^* on our arbitrarily chosen parameters is not unexpected given that the value of the fixed point itself is not universal. For a highly similar example see section 12.5.3 of [15]. In order to extract exponents we solve the eigenvalue equation given by linearizing these equations near each fixed point. The linearized matrix is

$$\mathcal{M} = \begin{bmatrix} 2 - \frac{6Vg^*}{(\Lambda^2+r^*)^2} & \frac{6V}{\Lambda^2+r^*} \\ \frac{24V(g^*)^2}{(\Lambda^2+r^*)^3} & 4 - d - \frac{24Vg^*}{(\Lambda^2+r^*)^2} \end{bmatrix},$$

and we can plug in the Gaussian and nontrivial fixed point values of r^* and g^* to obtain

$$\mathcal{M}_{\text{Gauss}} = \begin{bmatrix} 2 & \frac{6V}{\Lambda^2} \\ 0 & 4-d \end{bmatrix} \tag{4.75}$$

and

$$\mathcal{M}_{\text{Crit}} = \begin{bmatrix} d/2 & (8-d)\frac{3V}{2\Lambda^2} \\ \frac{(4-d)^2}{8-d}\frac{2\Lambda^2}{3V} & d-4 \end{bmatrix}. \tag{4.76}$$

The matrix in Eq.(4.75) is triangular, and thus the eigenvalues can be read off directly as $\lambda = (2, 4-d)$. In $d = 3$ the largest is 2 and thus as per Eq.(2.50) $\nu = 1/2$. Since $A = 0$ in Eq.(4.23) the anomalous dimension is $\eta = 0$, giving mean field results as expected. At the other fixed point, however, $\eta = 0$ for the same reason, but we must solve the eigensystem corresponding to Eq.(4.76) starting with the characteristic equation

$$0 = (d/2 - \lambda)(d - 4 - \lambda) - (4 - d)^2, \tag{4.77}$$

which is clearly independent of V and Λ as expected. The eigenvalues are thus

$$\lambda_\pm = \frac{1}{4}\Big(3d - 8 \pm \sqrt{17d^2 - 144d + 320}\Big) \tag{4.78}$$

and λ_+ gives the mean field value of 2 in both $d = 2$ and $d = 4$, the former being particularly surprising as the Onsager exponents for the full φ^4 theory in $d = 2$ have $\eta = 1/4$ much larger than in the $d = 3$ case. Interpreting the action in Eq.(4.26) as a subset of the full φ^4 theory, this seems to indicate that the neglected terms contribute *all* of the mean-field-deviating behavior of the $d = 2$ system. It is important to clarify that this 'subset' interpretation is just a heuristic analysis at this point, but such interpretations are worth exploring due to the possibility that they may reveal to what extent η and ν affect each other given a particular universality class. In contrast, something fundamentally different occurs in $d = 3$, where this reduced action contributes to deviations from mean field.

In particular for $d = 3$ we find that

$$\begin{aligned} \lambda_+ &= \frac{1}{4}(1 + \sqrt{41}) && (4.79)\\ \Rightarrow \nu &= \frac{4}{1 + \sqrt{41}} && (4.80)\\ &= \frac{1}{2} + \frac{1}{10}(\sqrt{41} - 6), && (4.81) \end{aligned}$$

where the last line extracts the decimal part of the irrational and shows the difference from mean field. The numerical value $\nu \approx 0.540$ is larger than mean filed theory but smaller than the φ^4 critical value. Regardless, this fixed point is clearly not mean field and we give a list of exponents in Table 4.1 as well as numerical approximations for them.

It is important to note that although the action here is not that of φ^4 theory, the method of the limit of finite systems can produce exact exponents as it has here.

Table 4.1: Critical exponents of the reduced φ^4 theory in Eq.(4.26) corresponding to the nontrivial fixed point in $d = 3$. These exponents lie between the φ^4 critical exponents and those of mean field theory. They are closed form exact values for the system given in Eq.(4.26).

Exponent	Exact	Approximate
α	$\frac{1}{2} - \frac{3}{10}(\sqrt{41} - 6)$	0.379
β	$\frac{1}{4} + \frac{1}{20}(\sqrt{41} - 6)$	0.270
γ	$1 + \frac{1}{5}(\sqrt{41} - 6)$	1.08
δ	5	5
ν	$\frac{1}{2} + \frac{1}{10}(\sqrt{41} - 6)$	0.540
η	0	0

Chapter 5

Concluding Remarks

Despite the focus of this thesis on classical φ^4 theory, the work herein should not be considered specialized methods for this model but rather research on general nonperturbative analytic techniques to calculate physical observables in field theory. The use of φ^4 theory is as a 'fruit-fly model for phase transitions' [23] in that it is the simplest interacting model with nontrivial critical behavior and as such it makes for an excellent proving ground for new techniques. Given the initial progress shown here by the methods above, the next natural direction to take, after further refinement of the work in Chapter 4, is application of these methods to quantum quartic models and higher order interaction terms of the same type: semi-local reflection-symmetric models both with and without disorder. The benefits of a general nonperturbative technique for calculating observables in interacting quantum field theories is hard to overstate. Therefore any hint of potential success toward that goal, big or small, should garner continued interest. This thesis has been written for an audience with the intention of near-future application for further research.

Appendix A

The nonlinear eigenvalue equation from which we generate our basis is

$$\nabla^2\varphi - r\varphi - g\varphi^3 = 0, \tag{A.1}$$

where $\varphi = \varphi(\mathbf{x})$, r is the mass coefficient, and g is the coupling. This is readily recognized as the d-dimensional anharmonic oscillator equation. We begin by choosing an anzatz solution $\varphi(\mathbf{x}) = A\mathrm{pq}(\mathbf{k}\cdot\mathbf{x} + \theta, m)$, where pq is a Jacobi elliptic function from Table A.1 and $\theta = 0$ or $\theta = K(m)$. Inserting this anzatz into Eq.(A.1) produces a set of equations

$$0 = (k^2 q_2 - r)A\mathrm{pq}(\mathbf{k}\cdot\mathbf{x} + \theta, m) \tag{A.2}$$

$$0 = (A^{-2}k^2 q_4 - g)A^3\mathrm{pq}^3(\mathbf{k}\cdot\mathbf{x} + \theta, m) \tag{A.3}$$

that must vanish separately, where both q_2 and q_4 are chosen according to pq via Table A.1.

Table A.1: The Jacobi elliptic functions and the values corresponding to differential equations they solve. m is the elliptic modulus. This list is reproduced from [24].

pq	q_2	q_4
sn	$-(1+m^2)$	m^2
cn	$2m^2-1$	$-m^2$
dn	$2-m^2$	-1
ns	$-(1+m^2)$	1
nc	$2m^2-1$	$1-m^2$
nd	$2-m^2$	m^2-1
sd	$2m^2-1$	$-m^2(1-m^2)$
ds	$2m^2-1$	1
cd	$-(1+m^2)$	m^2
dc	$-(1+m^2)$	1
sc	$2-m^2$	$1-m^2$
cs	$2-m^2$	1

Since $\mathrm{pq}(\mathbf{k}\cdot\mathbf{x} + \theta, m) \neq 0$ in general we are left with algebraic equations

$$r = k^2 q_2 \tag{A.4}$$

$$A^2 g = k^2 q_4, \tag{A.5}$$

which we can use to solve for m and A once we choose pq. Parameter $\mathbf{k}$, on the other hand, will be determined by applying periodic boundary conditions

$$\varphi(x_i = L) = \varphi(x_i = 0) \; \forall \; i \in \{1, 2, \ldots, d\} \tag{A.6}$$

$$\frac{\partial \varphi(x_i = L)}{\partial x_i} = \frac{\partial \varphi(x_i = 0)}{\partial x_i} \; \forall \; i \in \{1, 2, \ldots, d\} \tag{A.7}$$

to the eigenproblem

$$\nabla^2 \varphi - r\varphi - g\varphi^3 = \lambda \varphi \tag{A.8}$$

where L is the characteristic size of the system. The allowed values of $\mathbf{k}$ for this boundary value problem are

$$\mathbf{k_n} = \frac{2K(m)\mathbf{n}}{L} \tag{A.9}$$

for $\mathbf{n} = (n_1, \ldots, n_d)$ with integers for each n_i. Recall that $K(m)$ is the quarter period of the Jacobi elliptic functions, so these allowed values simply state that only half-period multiples will satisfy periodic boundary conditions. The corresponding eigenvalue becomes

$$\lambda_{\mathbf{n}} = -k_{\mathbf{n}}^2 q_2 - r, \tag{A.10}$$

which gives the expected relation $\lambda_{\mathbf{n}} = k_{\mathbf{n}}^2 - r$ in the $g \to 0$ limit since $q_2(m = 0) = -1$ for both sn and cn. Eqn's (A.5), (A.9), and (A.10) don't quite uniquely determine the eigensystem since the equation for $E_{\mathbf{n}}$ is identical with the equation for r for the eigenproblem. In order to obtain unique eigenstates we must normalize them. If we write down a typical expression to normalize these eigenfunctions

$$1 = A^2 \int_0^L d^d x \mathrm{pq}^2(\mathbf{k_n} \cdot \mathbf{x}, m) \tag{A.11}$$

we find that A or m or both could be $\mathbf{n}$ dependent scalars in general. In order to determine the exact depen-

dence we will impose the restriction that in the limit that $g \to 0$ we reproduce the normalized eigensystem for the free case (i.e. $A \to \sqrt{2/L}$). We find that m depends on $\mathbf{n}$. We can now state the full eigensystem solution by restricting to $m \in (0,1)$ and the Jacobi function pq corresponding to the appropriate range of r and g. In particular we find

$$\begin{aligned} \varphi_n &= A(m_{\mathbf{n}})\mathrm{sn}(\mathbf{k_n}\cdot\mathbf{x}, m_{\mathbf{n}}) && \text{(A.12)} \\ A(m) &= \sqrt{\frac{2}{L}}\left(\frac{2K(m) - E(am(2K(m),m),m)}{m^2 K(m)}\right)^{-1/2} && \text{(A.13)} \\ \lambda_n &= (m_{\mathbf{n}}^2+1)k_{\mathbf{n}}^2 - r && \text{(A.14)} \end{aligned}$$

for the sn case and

$$\begin{aligned} \varphi_n &= A(m_{\mathbf{n}})\mathrm{cn}(\mathbf{k_n}\cdot\mathbf{x}, m_{\mathbf{n}}) && \text{(A.15)} \\ A(m) &= \sqrt{\frac{2}{L}}\left(\frac{2(1-m^2)K(m) - E(am(2K(m),m),m)}{m^2 K(m)}\right)^{-1/2} && \text{(A.16)} \\ \lambda_n &= (2m_{\mathbf{n}}^2-1)k_{\mathbf{n}}^2 - r && \text{(A.17)} \end{aligned}$$

for the cn case. Here $E(x,m)$ is the complete elliptic function of the second kind and $am(x,m)$ is the amplitude function. Notice that in these equations $m = m(\mathbf{n})$ which is determined for each $\varphi_{\mathbf{n}}$ by self-consistent solution of

$$A(m_{\mathbf{n}})^2 g = k_{\mathbf{n}}^2 q_4(m_{\mathbf{n}}). \qquad \text{(A.18)}$$

We are interested in showing that these solutions form a complete basis for all physically reasonable functions (in more formal math language we will prove that the eigensystem solution set forms a basis on $L_2(0,1)$)! This is a very bold claim and the recipe will be incomplete if we stop with just the solved eigensystem, but we will discuss more of this further below. We begin by looking at the trigonometric series expansion of the Jacobi elliptic functions. The only possible bounded trig functions that satisfy our periodic boundary of length L are

$$\begin{aligned} &\sin(\pi\mathbf{n}\cdot\mathbf{x}/\mathrm{L}) && \text{odd functions} && \text{(A.19)} \\ &\sin(\pi\mathbf{n}\cdot\mathbf{x} + \pi/2) && \text{even functions.} && \text{(A.20)} \end{aligned}$$

We could instead use cos to define the even and odd trig functions here, but the important point is that one type of trig function can be used to define all of the solutions allowed on a periodic boundary. These are exactly the terms appearing in the Jacobi trig expansion for sn (or for cn when using cos). They are also the Fourier expansion modes for this system, which form a complete basis for any function on $L_2(0,1)$. For the rest of the proof we will assume we are looking at a system in which $r \in (-\infty, \infty)$ and $g \in [0, \infty)$. Applying these restrictions to Eq.(A.18) and using Table A.1 we can see that the restriction to positive g eliminates the use of cn functions. Further requiring bounded functions effectively reduces the choice to sn solutions. Finally, we will ignore overall constant solutions, although including them in the analysis is trivial. If we suppose that an arbitrary function on $L_2(0, L)$ has the Fourier expansion

$$u(\mathbf{x}) = \sum_{\mathbf{j}} c_{o,\mathbf{j}} \mathrm{sin}(\pi \mathbf{n} \cdot \mathbf{x}/\mathrm{L}) + \mathrm{c}_{\mathrm{e},\mathbf{j}} \mathrm{sin}(\pi \mathbf{n} \cdot \mathbf{x}/\mathrm{L} + \pi/2), \tag{A.21}$$

then all we need to do is show that there is a one-to-one correspondence between the Fourier coefficients and the coefficients of an expansion of the same arbitrary function over the elliptic eigenstates

$$u(\mathbf{x}) = \sum_{\mathbf{j}} b_{o,\mathbf{j}} \mathrm{sn}(2K(m_{\mathbf{j}})\mathbf{j} \cdot \mathbf{x}/L, m_{\mathbf{j}}) + b_{e,\mathbf{j}} \mathrm{sn}(2K(m_{\mathbf{j}})\mathbf{j} \cdot \mathbf{x}/L + 2K(m_{\mathbf{j}}), m_{\mathbf{j}}). \tag{A.22}$$

This is easily done, however, via proof by induction. First we note that we only need to prove that either the odd or the even part of $u(\mathbf{x})$ has a complete basis description, since it follows that the other part can be constructed in exactly the same procedure. We look at the odd part only below and drop the o and e indices. Also, denote the trig expansion of a given eigenfuntion as

$$\varphi_{\mathbf{j}}(\mathbf{x}) = \sum_{\mathbf{j}} a_{\mathbf{j},n} \mathrm{sin}\left((2\mathrm{n}+1)\pi \mathbf{j} \cdot \mathbf{x}/\mathrm{L}\right). \tag{A.23}$$

Since n is a scalar the only trigonometric functions that can contribute to a given $\varphi_{\mathbf{j}}$ are those that have $\mathbf{j}$ lie on a line that passes through the origin and $\mathbf{j}$, thus we can restrict the calculation to one such line and drop the vector index notation. Further notice that due to the $2n+1$ indexing in the trig expansion, the even j indexed eigenfunctions are independent of the odd j indexed ones. Therefore we can WLOG further restrict the proof to the odd j indexed eigenfunctions, which we do below. Both of these simplifications are related to the partial orthogonality relations that the elliptic basis functions share, as detailed in Chapter 3. For the base case we see that in Eq. (A.23) the lowest eigenfunction φ_1 is the only eigenfunction containing the lowest Fourier mode $\mathrm{sin}(\pi \mathrm{x}/\mathrm{L})$. Thus we have an algebraic constraint equation

$$a_{1,1}b_1 = c_1, \tag{A.24}$$

that uniquely specifies the $j = 1$ eigenfunction amplitude via solving for b_1. Now we can proceed in the exact same way for the second lowest ($j = 3$) eigenfunction since the total φ_1 amplitude $a_{1,3}b_1$ has already been solved!

$$a_{3,3}b_3 = c_3 - a_{1,3}b_1, \tag{A.25}$$

which solves b_3. In this way, when we reach the j eigenfunction, the previous $j - 1$ eigenfunctions already have set amplitudes, so we simply solve the algebraic equation

$$a_{j,j}b_j = c_j - a_{1,j}b_1 - a_{3,j}b_3 - ... - a_{1,j-1}b_{j-1}, \tag{A.26}$$

for the one remaining variable b_j. QED

Thus we see that for any given arbitrary function on $L_2(0, 1)$ there is a unique representation of that function in terms of the eigensystem of Jacobi elliptic functions that solve our nonlinear model.

References

[1] E. Abrahams and Q. Si. Quantum criticality in the iron pnictides and chalcogenides. *Journal of Physics Condensed Matter*, 23(22):223201, June 2011.

[2] J. Bardeen, L. N. Cooper, and J. R. Schrieffer. Theory of superconductivity. *Phys. Rev.*, 108:1175–1204, Dec 1957.

[3] L. Bartosch, M. de Souza, and M. Lang. Scaling theory of the mott transition and breakdown of the grüneisen scaling near a finite-temperature critical end point. *Phys. Rev. Lett.*, 104:245701, Jun 2010.

[4] R. Benzi, G. Martinelli, and G. Parisi. Anomalous dimensions from a high temperature expansion without a lattice. *Physics Letters B*, 64(4):451–453, 10 1976.

[5] S. M. Bhattacharjee and A. Khare. Fifty years of the exact solution of the two-dimensional Ising model by Onsager. *Curr. Sci.*, 69:816–820, 1995. [Erratum: Curr. Sci.71,493(1996)].

[6] C. G. Callan. Broken scale invariance in scalar field theory. *Phys. Rev. D*, 2:1541–1547, Oct 1970.

[7] C. Castellani, C. D. Castro, D. Feinberg, and J. Ranninger. New model hamiltonian for the metal-insulator transition. *Phys. Rev. Lett.*, 43:1957–1960, Dec 1979.

[8] T.-P. Choy, R. G. Leigh, and P. Phillips. Hidden charge-2e boson: Experimental consequences for doped mott insulators. *Phys. Rev. B*, 77:104524, Mar 2008.

[9] M. A. Continentino. Universal behavior in heavy fermions. *Phys. Rev. B*, 47:11587–11590, May 1993.

[10] B. D. Craven. Stone's theorem and completeness of orthogonal systems. *Journal of the Australian Mathematical Society*, 12:211–223, 5 1971.

[11] NIST Digital Library of Mathematical Functions. http://dlmf.nist.gov/, Release 1.0.11 of 2016-06-08. Online companion to [27].

[12] S. El-Showk, M. F. Paulos, D. Poland, S. Rychkov, D. Simmons-Duffin, and A. Vichi. Solving the 3d ising model with the conformal bootstrap ii. $$c$$ c -minimization and precise critical exponents. *Journal of Statistical Physics*, 157(4):869–914, 2014.

[13] M. P. A. Fisher, P. B. Weichman, G. Grinstein, and D. S. Fisher. Boson localization and the superfluid-insulator transition. *Phys. Rev. B*, 40:546–570, Jul 1989.

[14] H. A. Gersch and G. C. Knollman. Quantum cell model for bosons. *Phys. Rev.*, 129:959–967, Jan 1963.

[15] N. Goldenfeld. *Lectures on Phase Transitions and the Renormalization Group*. Westview Press, 1992.

[16] G. R. Golner. Nonperturbative renormalization-group calculations for continuum spin systems. *Phys. Rev. B*, 33:7863–7866, Jun 1986.

[17] Hegg, Anthony and Phillips, Philip W. Strongly coupled fixed point in φ^4 theory. *EPL*, 115(2):27005, 2016.

[18] J. Hubbard. Electron correlations in narrow energy bands. *Proceedings of the Royal Society of London A: Mathematical, Physical and Engineering Sciences*, 276(1365):238–257, 1963.

[19] L. P. Kadanoff, W. Götze, D. Hamblen, R. Hecht, E. A. S. Lewis, V. V. Palciauskas, M. Rayl, J. Swift, D. Aspnes, and J. Kane. Static phenomena near critical points: Theory and experiment. *Rev. Mod. Phys.*, 39:395–431, Apr 1967.

[20] R. Kenna. Universal scaling relations for logarithmic-correction exponents. In Y. Holovatch, editor, *Order, Disorder and Criticality: Advanced Problems of Phase Transition Theory Volume III*. World Scientific Publishing Co., 2013.

[21] H. Kleinert and V. Schulte-Frohlinde. *Critical Properties of φ^4-Theories*. World Scientific, 2001.

[22] J. M. Kosterlitz and D. J. Thouless. Ordering, metastability and phase transitions in two-dimensional systems. *Journal of Physics C: Solid State Physics*, 6(7):1181, 1973.

[23] D. P. Landau and K. Binder. *A Guide to Monte Carlo Simulations in Statistical Physics*. Cambridge University Press, second edition, 2005. Cambridge Books Online.

[24] P. Liang and J. Liang. Jacobi elliptic function solutions to $(1 + 1)$ dimensional nonlinear schrdinger equation in management system. *Optik - International Journal for Light and Electron Optics*, 122(14):1289 – 1292, 2011.

[25] A. J. Millis. Effect of a nonzero temperature on quantum critical points in itinerant fermion systems. *Phys. Rev. B*, 48:7183–7196, Sep 1993.

[26] Y. Nakai, T. Iye, S. Kitagawa, K. Ishida, H. Ikeda, S. Kasahara, H. Shishido, T. Shibauchi, Y. Matsuda, and T. Terashima. Unconventional Superconductivity and Antiferromagnetic Quantum Critical Behavior in the Isovalent-Doped $BaFe_2(As_{1-x}P_x)_2$. *Physical Review Letters*, 105(10):107003, Sept. 2010.

[27] F. W. J. Olver, D. W. Lozier, R. F. Boisvert, and C. W. Clark, editors. *NIST Handbook of Mathematical Functions*. Cambridge University Press, New York, NY, 2010. Print companion to [11].

[28] L. Onsager. Crystal statistics. i. a two-dimensional model with an order-disorder transition. *Phys. Rev.*, 65:117–149, Feb 1944.

[29] R. Pathria and P. Beale. *Statistical Mechanics*. Elsevier Science, 1996.

[30] P. Phillips. Fractionalize this. *Nature Physics*, 6(12):931–933, 12 2010.

[31] P. Ramond. *Field Theory: A Modern Primer*. The Benjamin/Cummings Publishing Company, Inc., 1981.

[32] R. Rattazzi, V. S. Rychkov, E. Tonni, and A. Vichi. Bounding scalar operator dimensions in 4 d cft. *Journal of High Energy Physics*, 2008(12):031, 2008.

[33] G. R. Stewart. Non-fermi-liquid behavior in d- and f-electron metals. *Rev. Mod. Phys.*, 73:797–855, Oct 2001.

[34] I. M. Suslov. Divergent perturbation series. *Journal of Experimental and Theoretical Physics*, 100(6):1188–1233, 2005.

[35] K. Symanzik. Small distance behaviour in field theory and power counting. *Communications in Mathematical Physics*, 18(3):227–246, 1970.

[36] D. D. Vvedensky. Lecture notes in coarse-grained theory of surface nanostructure formation. `http://www.lorentzcenter.nl/lc/web/2010/404/presentations/VvedenskyI_4.pdf`, August 2010. [Online; accessed 4-September-2016].

[37] P. Walmsley, C. Putzke, L. Malone, I. Guillamón, D. Vignolles, C. Proust, S. Badoux, A. I. Coldea, M. D. Watson, S. Kasahara, Y. Mizukami, T. Shibauchi, Y. Matsuda, and A. Carrington. Quasiparticle Mass Enhancement Close to the Quantum Critical Point in $BaFe_2(As_{1-x}P_x)_2$. *Physical Review Letters*, 110(25):257002, June 2013.

[38] B. Widom. Some topics in the theory of fluids. *The Journal of Chemical Physics*, 39(11):2808–2812, 1963.

[39] K. G. Wilson. Renormalization group and critical phenomena. i. renormalization group and the kadanoff scaling picture. *Phys. Rev. B*, 4:3174–3183, Nov 1971.

[40] K. G. Wilson. Renormalization group and critical phenomena. ii. phase-space cell analysis of critical behavior. *Phys. Rev. B*, 4:3184–3205, Nov 1971.

[41] K. G. Wilson. The renormalization group: Critical phenomena and the kondo problem. *Rev. Mod. Phys.*, 47:773–840, Oct 1975.

[42] K. G. Wilson and M. E. Fisher. Critical exponents in 3.99 dimensions. *Phys. Rev. Lett.*, 28:240–243, Jan 1972.

[43] K. G. Wilson and J. Kogut. The renormalization group and the expansion. *Physics Reports*, 12(2):75 – 199, 1974.

[44] W. P. Wolf. The Ising model and real magnetic materials. *Brazilian Journal of Physics*, 30:794 – 810, 12 2000.